Icarus 268 (2016) 295–312

Contents lists available at ScienceDirect

Icarus

journal homepage: www.journals.elsevier.com/icarus

Effect of a single large impact on the coupled atmosphere-interior evolution of Venus

Cédric Gillmann [a,*], Gregor J. Golabek [b,c], Paul J. Tackley [b]

[a] Royal Observatory of Belgium, Avenue Circulaire 3, 1180 Uccle, Belgium
[b] Institute of Geophysics, ETH Zurich, Sonneggstrasse 5, 8092 Zurich, Switzerland
[c] Bayerisches Geoinstitut, Universität Bayreuth, Universitätstrasse 30, 95440 Bayreuth, Germany

ARTICLE INFO

Article history:
Received 6 July 2015
Revised 19 October 2015
Accepted 2 December 2015
Available online 21 December 2015

Keywords:
Venus, interior
Venus, atmosphere
Impact processes
Volcanism
Atmospheres, evolution

ABSTRACT

We investigate the effect of a single large impact either during the Late Veneer or Late Heavy Bombardment on the evolution of the mantle and atmosphere of Venus. We use a coupled interior/exterior numerical code based on StagYY developed in Gillmann and Tackley (Gillmann, C., Tackley, P.J. [2014]. J. Geophys. Res. 119, 1189–1217). Single vertical impacts are simulated as instantaneous events affecting both the atmosphere and mantle of the planet by (i) eroding the atmosphere, causing atmospheric escape and (ii) depositing energy in the crust and mantle of the planet. The main impactor parameters include timing, size/mass, velocity and efficiency of energy deposition. We observe that impact erosion of the atmosphere is a minor effect compared to melting and degassing triggered by energy deposition in the mantle and crust. We are able to produce viable pathways that are consistent with present-day Venus, especially considering large Late Veneer Impacts. Small collisions (<100 km radius) have only local and transient effects. Medium-sized impactors (100–400 km) do not have much more consequence unless the energy deposition is enhanced, for example by a fast collision. In that case, they have comparable effects to the largest category of impacts (400–800 km): a strong thermal anomaly affecting both crust and mantle and triggering melting and a change in mantle dynamics patterns. Such an impact is a global event and can be responsible for volcanic events focused at the impact location and near the antipode. Depending on the timing of the impact, it can also have major consequences for the long-term evolution of the planet and its surface conditions by either (i) efficiently depleting the upper mantle of the planet, leading to the early loss of its water or (ii) imposing a volatile-rich and hot atmosphere for billions of years.

1. Introduction

The surfaces of the terrestrial bodies show that impact craters are a common feature in the Solar System. That is especially true for the Moon, Mercury and Mars, but craters can also be found on Earth. Venus is certainly no exception, although the present-day surface of Venus displays a relatively small number of craters due to the young surface age of 300–1000 Ma (Schaber et al., 1992; Herrick, 1994; Strom et al., 1994; McKinnon et al., 1997). In fact, a large early collision is considered to be a possible reason for Venus' slow and retrograde rotation (Baines et al., 2013; Raymond et al., 2013). While the present-day surface of Venus gives us few definite clues about its past impact history, comparison with the Earth and the other terrestrial bodies and numerical simulations indicates that the terrestrial planets experienced early on an intense bombardment by all types of bodies ranging from small sizes to impactors on the 100 km scale or even larger. The final stages of Earth's accretion involved bodies with up to Mars' mass (Hartmann and Davis, 1975; Cameron and Ward, 1976; Canup and Asphaug, 2001; Canup, 2004) or even larger (Canup, 2012), while afterwards, impacting bodies tend to decrease in size, mass and frequency.

Geochemical data indicate that after the formation of both the Earth's Moon and the Earth's core siderophile elements must have been introduced via chondritic impactors into the Earth's mantle. This Late Veneer (LV) arises from the clearing of leftover planetesimals from planetary accretion declining for several hundred million years, typically occurring between the time of the Moon forming impact and 500 Ma after the start of the accretion (Raymond et al., 2013). Numerical simulations of the LV phase by Raymond et al. (2013) imply the delivery of a total mass around $9 \cdot 10^{-3}$ M_{Earth}. Jacobson et al. (2014) find a slightly lower value

* Corresponding author.
E-mail address: cedric.gillmann@observatoire.be (C. Gillmann).

http://dx.doi.org/10.1016/j.icarus.2015.12.024
0019-1035/

around $5 \cdot 10^{-3}$ M_{Earth}. Models by both Bottke et al. (2010) and Raymond et al. (2013) suggest that the majority of the LV material was delivered by a few large impactors with up to lunar-size. The results of Raymond et al. (2013) also show that during this epoch Venus must have accreted comparable amounts of material as did Earth.

After the end of the LV, an impact spike, the so-called Late Heavy Bombardment (LHB), occurred. It has been suggested that this spike is correlated with the change of orbital architecture of the giant planets occurring around 500 Ma after the start of the Solar System (Tsiganis et al., 2005; Levison et al., 2011) and ending around 3.8 Ga ago. The total mass of impact material during the LHB phase is controversial (Levison et al., 2001; Ryder, 2002; Dauphas, 2003; Bottke et al., 2007; Marty and Meibom, 2007; Frey, 2008; Jørgensen et al., 2009). Due to age uncertainties in crater counting the use of scaling laws can only provide estimates. However, a total mass of about 10^{-4} M_{Earth} was suggested by various authors (Levison et al., 2001; Gomes et al., 2005; Jørgensen et al., 2009; De Niem et al., 2012). Since models indicate that much of the impactor material comes from the asteroid belt, models using the size–frequency distribution of the present-day asteroid belt suggest that during this epoch most material was delivered by few larger impactors with up to a few hundred km size (e.g. Abramov and Mojzsis, 2009).

It is believed that impactors of ~500 km diameter affect the habitability of a planet since they boil away oceans, thus affecting water and surface conditions at the large scale. Zahnle et al. (2007) discuss a qualitative scenario for the outcome of such an impact. The short-term effects are cataclysmic, with the production of a rock vapor atmosphere of 100 bar of sublimated silicates. Surface temperatures can immediately (within a timescale of hours to days) reach very high values (~1000 K). However, heat is efficiently radiated into space. In the medium-term, a steam atmosphere is present, limiting heat loss to space at the top of the cloud layer. This way, surface temperatures can stay high for a few 10^3 years and liquid water cannot be sustained. The long-term effects of such an impact are, however, less certain. Possible climatic consequences of impacts through the release of volatiles into the atmosphere are important and complex (Solomon et al., 1999; Bullock and Grinspoon, 2001; Segura et al., 2013). In the particular case of Venus, the chemistry of the atmosphere would be largely influenced by an impact, affecting the regular greenhouse effect, but more importantly cloud formation and albedo changes (Segura et al., 2013). At the moment, however, the precise effects of an impact are still unclear.

Here we use the newly developed coupled mantle-atmosphere methodology presented by Gillmann and Tackley (2014) to study these uncertain long-term effects of large impacts occurring during the LV and LHB epoch. For this purpose we choose to neglect the more immediate effects of impacts described above and to work on long-lasting volatile and energy exchanges. Such an approach fits better with the rest of our numerical model, employing time steps around 10^4 years, whereas most of the effects described above tend to settle down on a 10^3 years timescale. Such a high time resolution would only be needed to study the climatic effects during the presence of a steam atmosphere. Additionally, most numerical simulations used to study the long-term evolution of terrestrial planets are not able to adjust to such quick changes or uncommon conditions (for example rock vapor is a very specific situation that has no consequence for the rest of the evolution) while the calculation time is acceptable.

The structure of the manuscript is as follows: In the next section we describe the coupled model, the applied impact heating model and the atmosphere erosion model. This is followed by a discussion of the model setup. The last three sections contain our findings, the discussion and the conclusions.

2. Model

2.1. Basic coupled model

Our model for the evolution of Venus encompasses various components that represent different aspects of the history of the planet. Here we focus on volatile exchange, as this appears to be the most important feature. The coupling is two-way. Mantle activity leads to degassing, releasing volatiles into the atmosphere and contributing to the greenhouse effect. On the other hand, the greenhouse effect governs the surface temperature, which acts as a boundary condition for mantle convection.

The model is composed of four different parts (Fig. 1): (i) the mantle convection model, (ii) the atmospheric escape module, (iii) the atmosphere model and (iv) the impact module. Part 4 will be described in more detail in a dedicated section below, as it is the latest extension. A detailed description of parts (i), (ii) and (iii) of the coupled model can be found in our previous work (Gillmann and Tackley, 2014). However, for completeness, we present here a brief summary.

Section (i) deals with mantle dynamics, melting and volcanic production. It is based on an adapted version of the state-of-the-art code StagYY (Tackley, 2008; Hernlund and Tackley, 2008). Specifically, we use the same model setup as Armann and Tackley (2012) for Venus, employ similar parameters and apply the same grid resolution in a 2D spherical annulus layout.

A compressible anelastic, infinite Prandtl number mantle is assumed. We solve the mass, momentum and energy conservation equations. Physical properties like density, thermal expansivity, and thermal conductivity are depth-dependent and are calculated as described in Tackley (1996, 1998). Radiogenic heating decays exponentially with time, based on Earth-like concentrations of heat producing elements (Janle et al., 1992; Turcotte, 1995; Nimmo and McKenzie, 1997). The phase transitions in the olivine system and in the pyroxene-garnet system are included as discussed in Xie and Tackley (2004).

The assumed rheology is viscous diffusion creep and plastic yielding (viscoplastic rheology). Diffusion creep parameters are based on laboratory experiments for the upper mantle (Karato and Wu, 1993) and other estimates for the lower mantle (Yamazaki and Karato, 2001). Viscosity is both temperature- and depth-dependent:

$$\eta(T, d) = \eta_0 \exp[(E + Bd)/(RT) - E/(RT_0)] \quad (1)$$

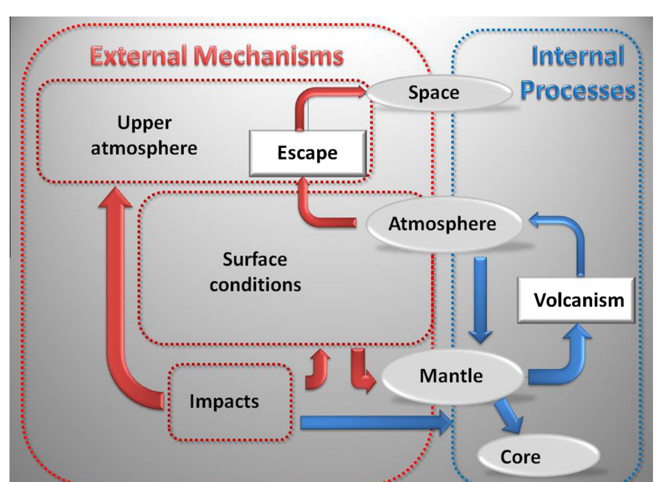

Fig. 1. Layout of the coupled model and interactions between the different parts described in the text.

with T being the absolute temperature, d the depth, E the activation energy, R the gas constant, and $B = \rho g V$ (related to the activation volume V), where g is the gravitational acceleration and ρ is a representative density for the region of interest. η_0 is the reference viscosity at temperature T_0 and zero pressure. Here we employ for η_0 a value of 10^{20} Pa s at $T_0 = 1600$ K. The models employs viscosity cutoffs at 6 orders of magnitude above and 10 orders of magnitude below the reference viscosity.

Plastic yielding is included with a constant ductile yield stress of 100 MPa following the preferred model of Armann and Tackley (2012). The surface and core–mantle boundaries are both free-slip and isothermal. The surface temperature is obtained from the atmosphere model. A core evolution model allows for its cooling over time and is detailed in Nakagawa and Tackley (2004).

Melting is treated as in other studies using the StagYY code (Nakagawa and Tackley, 2004, 2005, 2010; Nakagawa et al., 2009, 2010; Xie and Tackley, 2004; Armann and Tackley, 2012). After each time step, the temperature in each cell is compared to the depth-dependent solidus. If the temperature exceeds the solidus, melt is generated to bring the temperature back to the solidus, if sufficient basaltic end-member material is present. Only the basalt component can melt, which is approximated by a rapid increase in solidus temperature when all garnet and clinopyroxene has been removed by melting (McKenzie and Bickle, 1988). When melting occurs, all melt located above a certain depth (set to 600 km) is assumed to instantaneously erupt at the surface (Reese et al., 2007), since its migration can be considered to be fast compared to convection processes. When calculating degassing, we assume that 20% of the magma can contribute to degassing (Crisp, 1984; Bullock and Grinspoon, 1996; Reese et al., 2007). In our models, the concentration of volatiles in the melt scales linearly with the fraction of mantle mass that has already been melted. However Venus' volatile budget is uncertain, it is likely to be largely degassed at present-day (Grinspoon, 1993; Namiki and Solomon, 1998). Our simulations cover realistic volatile contents (see Table 2), using values from previous work (Grinspoon, 1993; Namiki and Solomon, 1998; Elkins-Tanton et al., 2007), as discussed in greater length in Gillmann and Tackley (2014).

Section (ii) deals with atmospheric escape, both thermal (hydrodynamic escape) and non-thermal. Hydrodynamic escape is very intense, but is relevant only during the early evolution of the planet (4–4.5 Ga ago). Our model uses work described in Gillmann et al. (2009). It is based on an energy-limited calculation of the linked escape of H and O in a water-rich atmosphere subjected to intense early extreme UV flux (EUV) from the Sun. Water is photo-dissociated into H and O. This module applies previous work by Kasting and Pollack (1983), Zahnle and Kasting (1986), Hunten et al. (1987) and Chassefière (1996a, 1996b).

During the later evolution (from 4 Ga ago until present-day) non-thermal escape mechanisms dominate the volatile removal from the atmosphere of Venus. We rely on observations and modeling to construct a non-thermal escape history for Venus. We consider mechanisms that rely on interactions between solar emission (extreme UV and solar wind) and the atmosphere (no surface processes or impact erosion). EUV decreases with time, reducing the efficiency of non-thermal escape mechanisms (Kasting et al., 1984; Zhang et al., 1993; Jakosky et al., 1994; Chassefière, 1996a, 1996b; Lammer et al., 2003a, 2003b; Kasting and Catling, 2003; Bauer and Lammer, 2004; Chassefière and Leblanc, 2004; Lundin and Barabash, 2004; Smith et al., 2004). We reconstruct past escape rates from the evolution of EUV flux (Ribas et al., 2005). Observational constraints based on ASPERA measurements point to a range from 10^{24} to 10^{25} s^{-1} for the present-day escape of O^+ at the conditions of solar minimum.

Section (iii) is needed to calculate the surface temperature evolution from the atmosphere content. The model is based on a modified version of a simple one-dimensional, vertical, radiative–convective atmospheric model by Phillips et al. (2001). The greenhouse gases are CO_2 and H_2O. The black body law is used to link the solar flux to the effective temperature of the planet (the temperature at which Venus should radiate at equilibrium). The temperature of the atmosphere at the surface is then determined by finding the value for which radiative and convective gradients and temperature all match. The faint young Sun hypothesis is taken into account, with luminosity assumed to increase linearly with time from initially about 70% of its present value at 4.5 Ga ago (Gough, 1981; Ribas et al., 2010). The effect of clouds is not modeled separately, which means they are assumed to be steady-state features.

2.2. Impact model

Impacts have three main effects on the evolution of a terrestrial planet (Pham et al., 2011; de Niem et al., 2012; Shuvalov et al., 2014): (i) they deliver volatiles to both its interior and atmosphere (Svetsov, 2007, 2011), (ii) erode part of the atmosphere (Melosh and Vickery, 1989; Vickery, 1990; Newman et al., 1999; Shuvalov, 2009; Hamano and Abe, 2010) and (iii) deposit a large amount of energy in the crust and mantle of the planet (Croft, 1982; Monteux et al., 2007). In this study, we focus on points (ii) and (iii). At this point we do not include (i). Volatile delivery would be most important during accretion and early phases of the evolution of planetary bodies. However, it introduces additional variables related to the composition of the impactor, impact mechanism and retention of the target and impactor material, that are not well constrained. Additionally, the resulting uncertainties make it difficult to estimate the effects of other mechanisms [(ii) and (iii)] with any precision or to establish guidelines for possible long-term global evolutions. As the results section shows, such an addition would not add any qualitative feature to the simulations as melt. Volatile delivery would then only modify how much gas is injected into the atmosphere without changing the general evolution significantly. Our simulations with different degassing estimations partly cover such variations.

As a starting point we study only single impacts, in order to be able to assess their effect on the large-scale and long-term evolution. Thus, we choose to work with the largest impactors we can expect during the LV and the LHB. After accretion ceases, these medium to large (>100 km) impacts are rare events, especially after the end of the LV phase. Scaling from the lunar records indicates that only ~1 impactor in the range of 400 km radius is to be expected during the LHB, while ~800 km impactors are extremely rare. In addition to size, other key parameters related to impacts are the density of the impactor and the impact velocity. The density of the impactor is usually considered to be around 2700 kg m^{-3} (i.e. Ivanov, 2001; Britt et al., 2002; Bottke et al., 2012; Pham, 2012). The impact velocity for the case of impacts on Earth usually ranges between 10 and 36 km s^{-1} (Gomes et al., 2005; Shuvalov, 2009; De Niem et al., 2012). Results by Raymond et al. (2013) indicate impact velocities for the case of Venus during the LV of up to $\sim 4 v_{esc}$ (~41 km s^{-1}) with a median value of $1.76 v_{esc}$ (~18 km s^{-1}). We employ a corresponding range for our calculations.

2.2.1. Erosion

During an impact, atmospheric erosion occurs when the velocity acquired by a portion of the atmospheric gas exceeds the planet's escape velocity. Atmospheric erosion by impacts occurs in several ways, as summarized in Fig. 2.

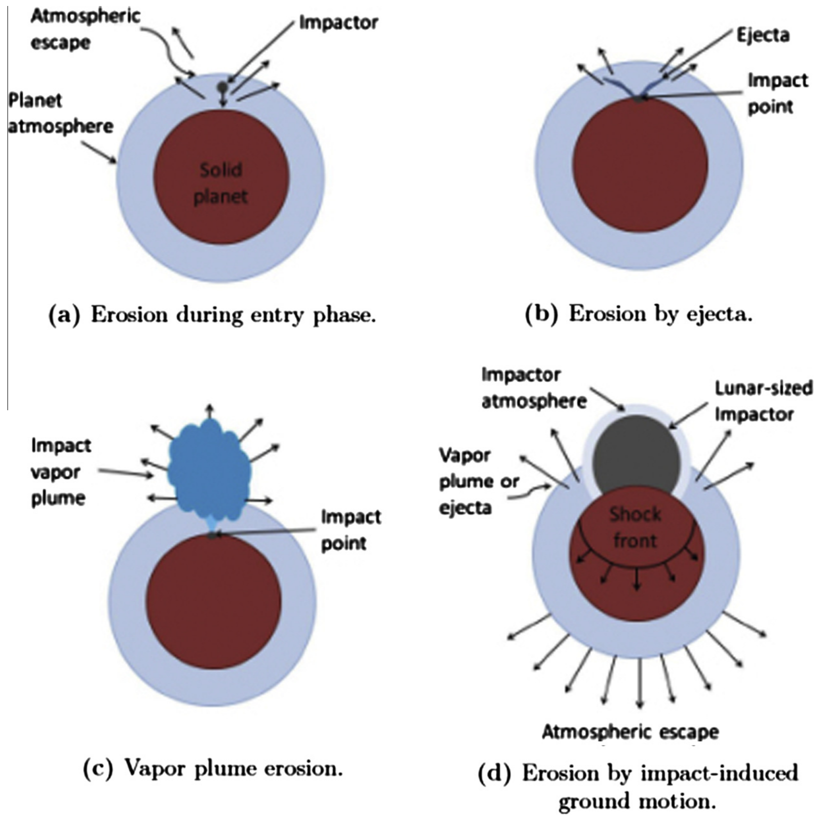

Fig. 2. Schematic representation of four different processes leading to the impact erosion of a terrestrial atmosphere (see text). Taken from Pham (2012).

(a) Erosion by compression occurs before the impact, when the impactor enters the atmosphere of the planet and creates a shockwave (Walker, 1986). The part of the atmosphere that escapes is accelerated by the rebound of the shockwave first driven downwards and then upwards. However this process is inefficient (Walker, 1986; Ahrens, 1993; Newman et al., 1999).
(b) The second type of erosion is caused by the solid impact ejecta. Loose material ejected from the crater at impact travels through the atmosphere and transfers part of its momentum to volatiles on its trajectory. It is also deemed to be inefficient (Melosh and Vickery, 1989; Ahrens, 1993).
(c) The rise of an impact-induced vapor plume can lead to more efficient erosion of the atmosphere (Melosh and Vickery, 1989), since a significant part of the kinetic energy from the impactor can be transferred and used to vaporize both impactor and target material, resulting in a vapor plume that generates a shockwave traveling upwards in the atmosphere. Its expansion can eject a significant part of the atmosphere.
(d) Finally, the fourth erosion process is erosion by ground motion, which is more significant for lunar-sized impacts (Ahrens, 1993; Chen and Ahrens, 1997; Genda and Abe, 2003). If the impactor has sufficient energy to generate a global shockwave in the solid planet focussing at the antipode of the impact site, energy can be transmitted to the atmosphere and lead to its escape. Genda and Abe (2003) estimate that up to 20% of the atmosphere of a planet could be removed this way by giant impacts. However older studies suggest that a Moon-sized impactor could even remove most of the early Earth's atmosphere (Cameron, 1983; Ahrens, 1993; Chen and Ahrens, 1997).

Work by Ahrens (1993) suggests significant removal of atmosphere by impactors on the 100 km scale range. However, more complete simulations using a sophisticated 3D version of the SOVA hydrocode (Shuvalov, 1999, 2009, 2010; Shuvalov et al., 2014) indicate inefficient atmosphere removal. SOVA is an Eulerian material response code with some Lagrangian features. It considers strong hydrodynamic flows with an accurate description of the boundaries between different materials (e.g., vapor, air, solid impactor, etc.). The governing transport equations consist of the conservation equations of mass, momentum and energy, which are solved for gas, liquid and solid materials, respectively.

In the first step, the Lagrangian equations are solved using a second-order difference scheme; in the second step, the data are remapped from the Lagrangian grid to the Eulerian grid with second order accuracy. In cases where the impactor is subjected to strong fragmentation, a two-step model approach was employed by Shuvalov et al. (2014). In the first step they used a 2D cylindrically symmetric grid (Shuvalov and Trubetskaya, 2007) to describe the processes of atmospheric entry, projectile deformation, fragmentation and deceleration. The 2D model allows for a very high-resolution grid of 40 cells per projectile radius along the central region. In the second step the output from the 2D model is taken as an initial data set for the 3D model.

Considering a large number of simulations covering the range of common parameters for impactors (size, incidence angle and velocity), Shuvalov (2009, 2010) provides a parameterized equation describing the efficiency of erosion by crater-forming impactors for sizes under $\sim$50 km radius with $1 < \xi < 10^7$ (Shuvalov, 2009) using:

$$\log_{10}\chi_a = -6.375 + 5.239(\log_{10}\xi) - 2.121(\log_{10}\xi)^2 + 0.397(\log_{10}\xi)^3 - 0.037(\log_{10}\xi)^4 + 0.0013(\log_{10}\xi)^5 \quad (2)$$

where the normalized atmospheric mass is given as

$$\chi_a = (m_a/M)v_{esc}^2/(V^2 - v_{esc}^2) \quad (3)$$

and

$$\xi = D^3\rho_i(V^2 - v_{esc}^2)/[H^3\rho_0 v_{esc}^2(\rho_p + \rho_i)] \quad (4)$$

is the efficiency of the erosion.

m_a is the mass of escaping air, M the mass of the impactor, v_{esc} is the escape velocity, V the impactor velocity, H the atmospheric scale height, D the impactor diameter, ρ_0 the atmosphere density at the surface, ρ_i the impactor density and ρ_p the planet's mean density.

Following Shuvalov (2009, 2010), it is possible to adapt the results to Venus and determine the efficiency of erosion of its atmosphere by impacts of different sizes. However experiments by Shuvalov (2009) focus on impacts smaller than 30 km.

Several issues arise. The first is that the law derived from the numerical experiments results is only strictly valid up to the 30–50 km diameter range. Due to the nature of the polynomial interpolation, exceeding the boundaries of validity tends to produce flawed results, leading to a reduced efficiency of erosion for larger impactors, mainly for impactors with >1000 km diameter (see Fig. 3).

For this reason we extrapolate the results for larger impactors linearly using the law described above. Several tests were made using different points where the extrapolation could start (using the last positive slope $dM_{atm\text{-}loss}/dR$ to compute a minimum impact erosion caused by larger impactors). Shuvalov et al. (2014) states that the law is valid at least up to 100 km diameter impactors. The erosion obtained with these cases varies only marginally and stays at levels expected from other estimations, like those based on tangent plane models (see Fig. 2 and 3).

The second issue is that more recent results (Shuvalov et al., 2014) tend to show that the equation underestimated the erosion of the atmosphere for fast impactors (at around 50 km/s), in this case fragmentation of the impactor has to be taken into account for smaller impactors (with <30 km diameter).

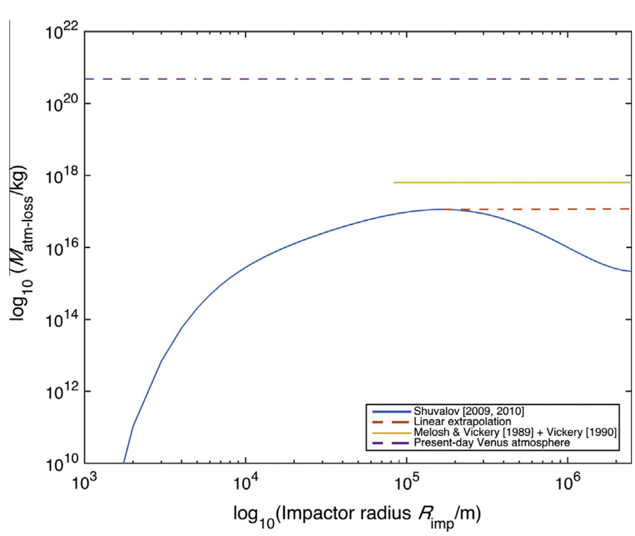

Fig. 3. Comparison of total atmosphere mass of Venus (violet) and impact erosion efficiency calculated from other works (Melosh and Vickery, 1989; Vickery, 1990; Shuvalov 2009, 2010), as a function of impactor diameter (blue and yellow). A linear extrapolation of the Shuvalov (2009, 2010) model is shown in red. Impact velocity is constant and assumed to be 36 km/s. The impact geometry is assumed to be head-on. (For interpretation of the references to color in this figure legend, the reader is referred to the web version of this article.)

However, it should be noted that for the larger impactor tested in the new models (100 km diameter), and with lower velocities (up to 30 km/s), the previous equation was effective at predicting the atmosphere erosion observed in the numerical models and yielded results at levels around 1% of the mass of the impactor (Shuvalov et al., 2014). We use large impactors, starting at the level tested by Shuvalov et al. (2014) and using velocities consistent with their experiments. Under those conditions, we use the law expressed in Shuvalov (2009, 2010) and extrapolate the law from 250 km diameter to larger values to obtain a minimum erosion rate.

Due to the uncertainty of the linear extrapolation, we also show results employing the tangent plane model for impactors (>50 km radius), leading to loss of all/most of the atmosphere above the plane (Melosh and Vickery, 1989; Vickery, 1990). This model uses a sector blow-off model with a focus on very efficient vapor plume escape. This process, and the simplified way it is implemented, overestimates (by roughly two orders of magnitude) the effect of atmospheric erosion compared to the more realistic numerical simulations of Shuvalov (2009) for vertical cases. For highly oblique cases, the differences are less pronounced; however, the tangent plane model is not applicable. Thus, escape via impact erosion seems to be quite inefficient, each single impactor removing only a fraction of its own mass, corresponding to a fraction of the total atmosphere of Venus (typically less than 1%), as confirmed by other studies considering the single impact scenario (Svetsov, 2000, 2007; Genda and Abe, 2003; Schlichting et al., 2015).

2.2.2. Mantle and dynamical effects

We use a simplified method to account for the temperature anomaly induced by the large impact in the mantle of Venus, following Monteux et al. (2007) and as used by Golabek et al. (2011). We neglect all effects that are not directly linked to the thermal anomaly, like silicate accretion, redistribution of Venus material displaced by the impact, crater excavation, etc.

At impact, an "isobaric core" is created (Croft, 1982) in which the temperature after the impact is nearly uniform. Its radius (R_{ic}) has been parameterized by Senshu et al. (2002):

$$R_{ic} = 3^{1/3}R_{imp} \quad (5)$$

Monteux et al. (2007) expressed the thermal anomaly linked to this isobaric core as function of planetary parameters and energy conversion efficiency. Here we adapted the equation for impact velocities larger than the escape velocity as suggested for collisions during the early evolution of the Solar System (e.g. Abramov and Mojzsis, 2009; Raymond et al., 2013).

$$\Delta T = (4/9)\pi * (\psi/F) * (\rho_p G R_p^2/c_p) * p_f \quad (6)$$

p_f is given as $p_f = (v_{imp}/v_{esc})^2$. Ψ is the efficiency parameter for the conversion of kinetic energy of the impactor into thermal energy. Its value is difficult to assess with any precision and varies between studies. O'Keefe and Ahrens (1977) use 0.3, while Shuvalov et al. (2014) calculate different values ranging between 0.4 and 0.6. We test a range of values covering these estimations. F represents the volume effectively heated normalized by the volume of the isobaric core. We use here the value of 2.7 as given by Monteux et al. (2007). Note that the temperature anomaly depends on the radius of the target body.

The thermal anomaly is superposed onto the pre-impact temperature field of the crust and mantle of Venus as calculated by the StagYY code. The center of the isobaric core is identical to the impact site. Outside the isobaric core, shock waves propagate and the peak pressure decays with the square of the distance r (Pierazzo et al., 1997). The thermal anomaly due to the impact is

Table 1
Parameters used in the reference Venus simulations.

Parameter	Symbol	Value (variation range)
Planetary radius	R	6052 km
CMB radius	R_{CMB}	3110 km
Mantle depth	D	2942 km
Gravity	g	8.87 m/s^2
Surface temperature (for uncoupled cases)	T_{surf}	740 K
Initial CMB temperature	T_{CMB_init}	4025 K
Specific heat capacity	c_p	1200 J/kg/K
Latent heat of melting	L	600 kJ/kg
Reference viscosity	η_{ref}	10^{20} Pa s ($\eta_{ref} - 2\eta_{ref}$)
Reference yield stress	τ_s	100 MPa (80–120 MPa)
Internal heating at present-day	$H_{present}$	5.2×10^{-12} W/kg
Internal heating at model start	H_{init}	18.77×10^{-12} W/kg
Half-life time of radiogenic heating	t_{half}	2.43 Ga
Solar irradiance (present-day)	S	2613.9 W/m^2
Initial CO_2 pressure	P_{CO2}	88.4 bar (0–95 bar)
Effective temperature	T_e	232 K
Reference oxygen escape rate (non-thermal; present-day)	E_{ref}	1.895×10^{24} s^{-1} ($0.6E_{ref} - 5E_{ref}$)
Energy deposition efficiency (hydrodynamic escape)	λ	2.4 (1.2–2.4)
Exospheric temperature (hydrodynamic escape)	T_{exo}	750 K (500–1250 K)
Hydrodynamic escape start	t_{h0}	10 Ma
Water concentration in lavas (present-day)	$[H_2O]_{l,p}$	50 ppmw (10–100 ppmw)
Impact time	t_i	100 Ma; 700 Ma (50–1600 Ma)
Impactor radius	R_{imp}	800 km; 400 km (50–800 km)
Efficiency of energy transfer to mantle	Ψ	0.6 (0.1–0.9)
Impactor velocity	v_{imp}	16 km/s (10–36 km/s)
Impactor density	ρ_i	2700 kg/m^3

assumed here to decrease following the parameterization from Senshu et al. (2002):

$$T(r) = \Delta T(R_{ic}/r)^{4.4} \quad (7)$$

With r being the distance from the impact site.

After the impact occurs and the thermal anomaly is included into the mantle temperature field in StagYY, no further modification is needed and the convection calculation proceeds using the modified temperature field. The code is stable even with a temperature anomaly of a few thousand Kelvin, although the time steps are greatly reduced during the first few million years following the event, given the large temperature gradient induced by the anomaly. Due to the high temperatures reached near the impact location, melting occurs immediately, leading to degassing, emplacement of basaltic crust and depletion of the upper mantle.

2.3. Simulation parameters

The main parameters we used for our simulations are listed in Table 1. The bulk of the experiments were performed using three sets of reference parameters (Ref, Ref1 and Ref2). We varied the following parameters: time of the impact (LHB, LV or variable), impactor size and mass, impact velocity and energy conversion efficiency. Each reference set of evolution contains 30 distinct simulations. An additional 30 simulations were performed with distinct sets of parameters differing from the reference cases, including rheology, degassing efficiency, volatile content, escape rates, and initial volatile content of the atmosphere. For comparison, corresponding models without an impact were run for those 20 cases that were not covered by previous work from Gillmann and Tackley (2014). 10 additional simulations were performed in which we varied the impact location (at a 90° angle from the standard impact point), and were based on the reference cases. They are used to determine whether features observed after the impact are linked to it or not. For comparison, 15 models used a constant surface temperature (i.e. no coupling with the atmosphere) for different main simulation parameters to investigate whether feedbacks played a part in phases affected by impact events. Hydrodynamic escape was employed in a subset of 10 models, although it only has a quantitative effect on early evolution and results presented here also apply to those cases.

The standard grid resolution was 512 × 128 cells with 1 million Lagrangian tracers (initially about 30 tracers/cell). 10 additional test cases with a higher grid resolution (512 × 256 cells) and with more tracers (100 tracers/cell) were performed and show no significant difference in the features discussed here: the exact timing of features differs marginally from the corresponding lower resolution cases, but are consistent among simulations. The main model features such as melt production, temperature variations, surface conditions, timing and length of the low surface temperature period or major mantle features linked to the impact are not significantly affected.

3. Results

3.1. Short-term effects of impacts

3.1.1. General features

Introducing impacts into the evolution of the planet adds a catastrophic event into a continuous history. As described above, the first most visible effect is the emplacement of a thermal anomaly in the crust and mantle. Examples of this anomaly are shown in Fig. 4. Due to the high temperature inside the isobaric core, the anomaly is thermally buoyant. Temperatures reached in the isobaric core are not dependent on the size of the impactor but on the size of the planet and on the collision velocity (see Eq. (6)).

After the emplacement of the buoyant anomaly, a stage of thermal relaxation occurs, where the hot zone flattens under the surface of the planet and widens. As noted by Monteux et al. (2007) this behavior is closely related to that of plumes reaching the upper mantle (Bercovici and Lin, 1996; Koch and Manga, 1996). The spreading of the anomaly depends on its size and temperature, thus dependent on size and velocity of the impactor. The initially hot isobaric core dissipates quickly and does not affect the mean mantle temperature for more than a few timesteps of

Table 2
Parameters used in model sets Ref, Ref1 and Ref2.

Parameter	Ref	Ref1	Ref2
Oxygen escape rate (non-thermal, present-day)	1.895×10^{24} s^{-1}	5.278×10^{24} s^{-1}	1.137×10^{24} s^{-1}
Water concentration (ppmw) initial/final[a]	150; 50	200; 100	100; 30
Initial water partial pressure (bar)	0.5	0.8	0.3
CO_2 concentration (ppmw) initial/final[a]	2000; 300	4000; 500	1000; 200

[a] Volatile composition of the lava is discussed in Gillmann and Tackley (2014).

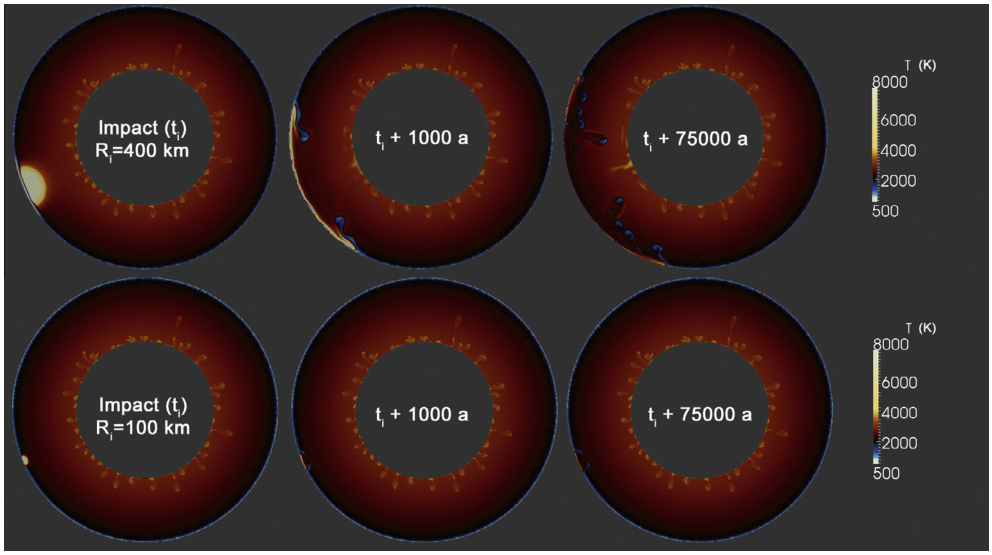

Fig. 4. Immediate effects on the mantle of Venus for an impactor with (upper panel) 400 km radius and (lower panel) with 100 km radius.

the simulation, except for the very high energy impacts, as shown in Fig. 4. Therefore, the global dynamics of the mantle is usually not immediately affected by the anomaly except that it can cause subduction and recycling of the crust and lithosphere in the region around the impact location. Smaller impact anomalies (like the 100 km radius one in Fig. 4) disappear on timescales of 10^4 a. In contrast, larger impactors (>400 km radius) cause spreading for several 10^5–10^6 a, although at a gradually decreasing rate. The extent of the spreading of the thermal anomaly due to a 100 km impactor corresponds to roughly twice its initial size, while a 400 km impactor anomaly spreads over 30% of the circumference of the planet and a 800 km impactor causes a global event. As a rule of thumb, impactors smaller than 200 km radius have mainly local effects occuring on a short timescale, while large impactors affect the planet as a whole with potentially lasting effects on the mantle and atmosphere.

High temperatures generated in the upper mantle and the spreading of the thermal anomaly lead to partial melting and the formation of new basaltic crust. For smaller impacts, the amount of melting is comparable to that of a minor volcanic event and leads to moderate volatile degassing. It corresponds to a small fraction of the total melt generated during the evolution (less than 1% of the volume of the mantle). Larger impacts, in particular the massive early 800 km scale objects, are able to melt a much larger volume of mantle, corresponding to up to 30% of the total melt volume generated during Venus' history.

This constitutes a significant, instantaneous, additional source of volatiles for the atmosphere (see Fig. 5). Due to the impact, CO_2 pressures can increase by a few percent. However the direct effect of this increase on surface temperature is marginal due to the presence of an already thick CO_2 atmosphere. Water partial pressure variations can have a larger effect on surface conditions, depending on the impact timing and the state of the atmosphere prior to the event (dry or wet). Sudden water release into a dry atmosphere by impactors larger than 200 km usually leads to an almost instantaneous temperature increase by up to 250 K.

In the case of a dry atmosphere, even small impacts can have observable consequences, with 50 km radius impactors causing an increase of 50–100 K above the dry-atmosphere temperature level (around 500 K).

In the case of a collision occurring during a wet atmospheric phase (especially the initial phase of high surface temperatures

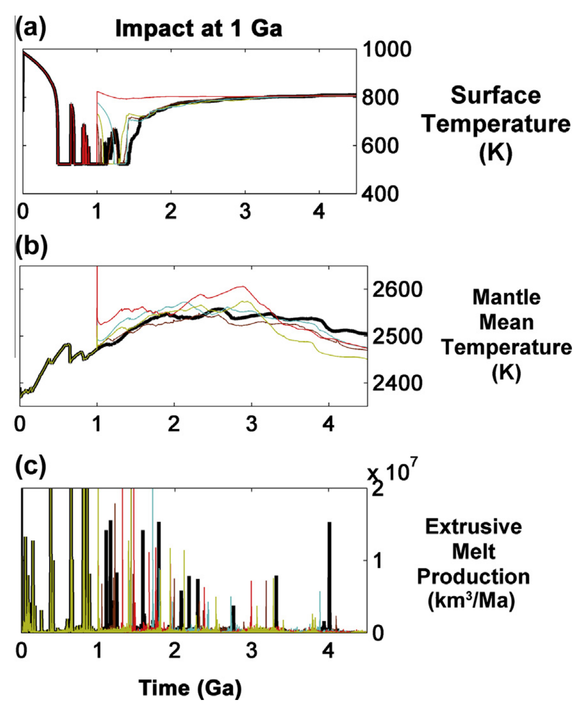

Fig. 5. Long-term evolution of (a) surface temperature, (b) mantle mean temperature and (c) melt production rate for an impact at 1 Ga, with an efficiency parameter of 0.6, a velocity of 36 km/s and different impactor sizes: 500 km radius (red; 68–26-Ref1), 300 km (blue; 68–13-Ref1), 200 km (yellow; 68–09-Ref1), 100 km (brown; 68–05-Ref1) and no impact (black; 68-Ref1). (For interpretation of the references to color in this figure legend, the reader is referred to the web version of this article.)

imposed by high initial water content), even large impacts will not modify the surface temperature significantly. Depending on the background water content of the atmosphere, a temperature increase by at most 10–50 K can be expected for impacts in the 400–800 km range.

Typical vertical profiles of the atmosphere of Venus are given in Fig. 1 of Gillmann and Tackley (2014), corresponding to a dry (but not devoid of water) atmosphere typical of present-day conditions, compared to a wet early atmosphere (3000 ppm water) leading to high surface temperatures. In the present-day situation, the tropopause extends to an altitude of 60 km, while in a wet atmosphere it can reach up to 90 km altitude. Vertical gradients are similar in both cases. Due to the highly idealized nature of the calculations, there is no difference between a post-impact high surface temperature case and a regular wet atmosphere case without an impact.

Depending on the time of the impact, the surface temperature modification can be brief or can extend until present-day. The defining parameter is the magnitude of the escape. The amount of volatiles released by collisions by impactors with <100 km radius can be removed by atmospheric escape over 1–50 Ma. On the other hand, large impacts (>400 km radius) can release much more volatiles. Atmospheric escape is strong enough to remove this excess water only during the first 500 Ma of the planetary evolution, resulting in higher surface temperatures in the longer-term.

3.1.2. Secondary parameters

As mentioned above, we tested the parameters affecting impact consequences, such as location, energy conversion efficiency and velocity. The location of the impact has been tested in different models, with the same impact occuring at the same time, with the same characteristics, but a 90° change in impact location (see Fig. 6). These cases allow us to distinguish between impact-related and non impact-related features in the long-term evolution. No qualitative change was observed in those models. Mean temperatures, surface conditions, melt production and mantle behavior are alike. Differences were insignificant and linked to the 2D annulus geometry of the simulations and the angular asymmetry of the amplitude of initial perturbations (resulting in asymmetry in plume formation). Thus, changing the impact location will affect different preexisting plumes and mantle structures. It is theoretically possible that due to complex interaction some particular cases might be more affected, but we have not found such a case among our simulations.

We also tested the effects of impact velocity and energy transfer efficiency (see Fig. 6). Both parameters have the same effects: their increase directly translates into increased energy deposition in the mantle and crust of the planet, causing higher temperatures in the thermal anomaly generated by the impact, but having no effect on the anomaly's initial size. Impact velocity increase has a stronger influence on the temperatures due to the squared relation (see Eq. (6)). Higher anomaly temperatures translate into deeper melting associated with the impact.

As such, parameters favoring higher temperatures (high efficiency, large impact velocity) will lead to a hotter anomaly, and will thus have a stronger effect on the mantle. Through this effect, they can enhance the amount of melting occuring. While the qualitative evolution of the models is not dependent on those parameters, improved energy deposition enhances the effects of the collision on the mantle and atmosphere. In the end, intermediate-sized impactors with extreme heating could affect the surface conditions as much as the larger bodies with more modest heating do. For slower impacts (velocity near the escape velocity of Venus) the temperature difference between the adiabatic core and ambient mantle is around 1000 K. For extreme cases with higher impact velocity a temperature rise by >8000 K can occur. For comparison, in the case of smaller targets, like Mars or the Moon, anomalies of 300–400 K for collision velocities near the respective escape velocities would be more common.

3.2. Middle-term effects: mantle features

Impacts with >100 km radius have been found to have lasting effects on the mantle of a planet like Venus. Smaller impacts have only local and limited consequences, without affecting the dynamics on the global scale. An animation of the evolution of mantle temperatures after a large (800 km radius impactor) collision is available as supplementary material. See Figs. 7a and 7b for snapshots displaying the mantle evolution after this large impact.

In general, simulations that have been subjected to a large impact show only a small increase in total melt production relative to simulations without impact events (only several percent of increase). However, the timing of melting episodes is modified.

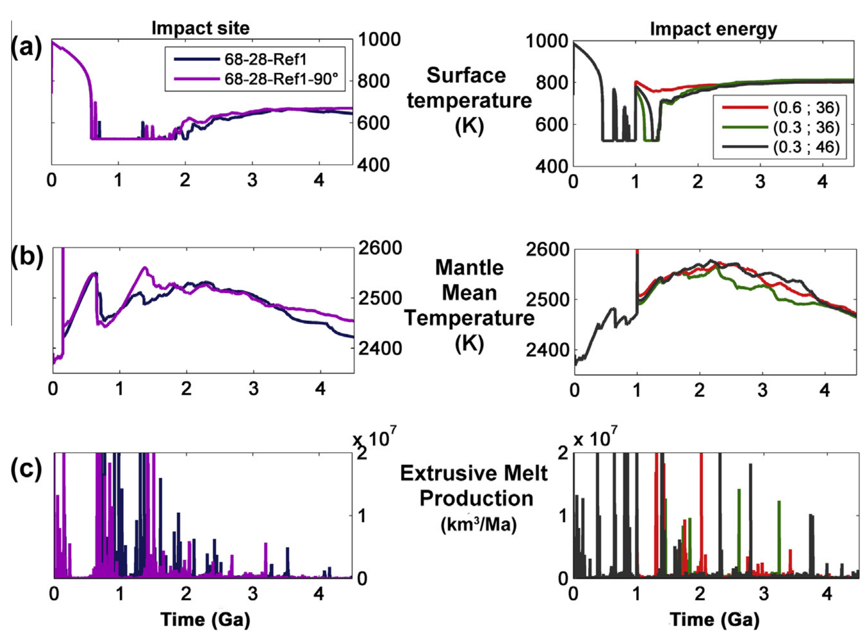

Fig. 6. Comparison of long-term evolution of (a) surface temperature, (b) mantle mean temperature and (c) melt production rate for (left) different impact locations (with a 800 km impactor, at 150 Ma, with an efficiency parameter of 0.6 and an impact velocity of 36 km/s; see Table 3) and (right) for different secondary impact parameters: kinetic energy transfer efficiency and impact velocity in km/s, with a 400 km impactor, 3.5 Ga ago, see Table 3: red is case 68–21-Ref1 (efficiency parameter of 0.6, velocity at 36 km/s), green is case 68–22-Ref1 (efficiency at 0.3, velocity at 36 km/s) and black is case 68–23-Ref1 (efficiency at 0.3, velocity at 46 km/s). (For interpretation of the references to color in this figure legend, the reader is referred to the web version of this article.)

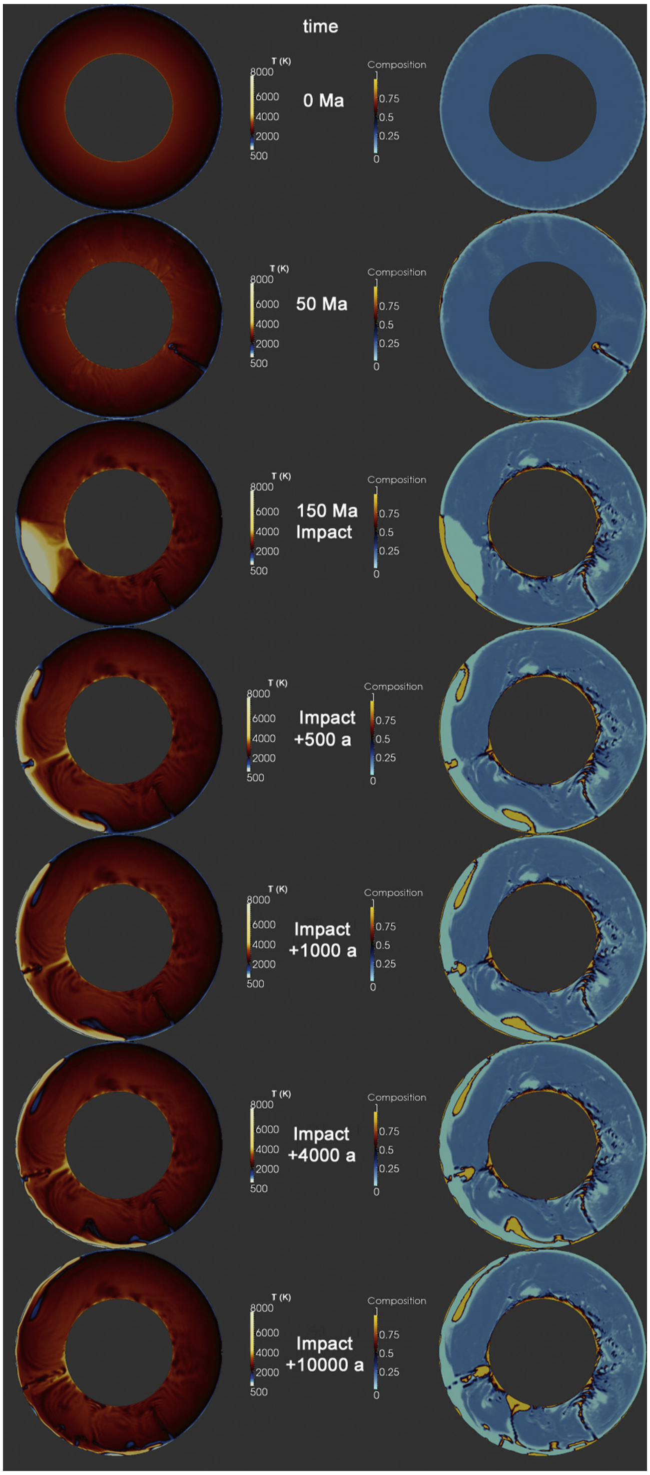

Fig. 7a. Evolution of venusian mantle temperature and mantle composition for case 68–28-Ref. with a 800 km radius impact occurring at 150 Ma with a conversion parameter of 0.6 and a velocity of 36 km/s. For composition, 0 stands for a depleted mantle and 1 for basaltic composition. Atmosphere coupling is taken into account.

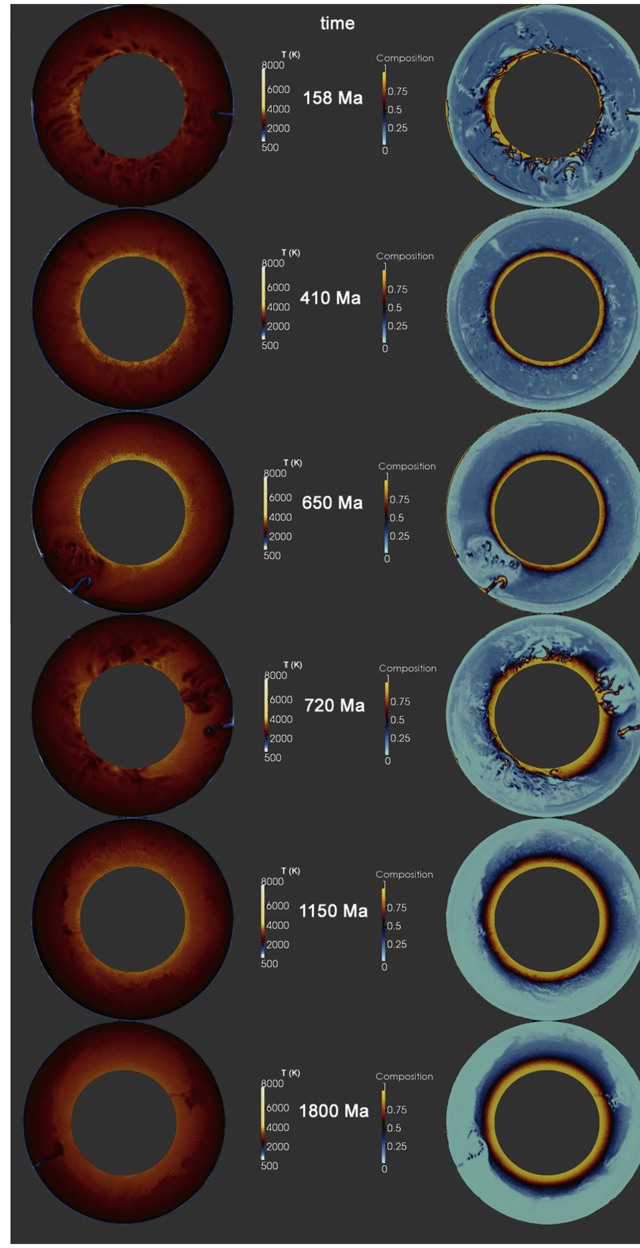

Fig. 7b. Long-term evolution of venusian mantle temperature and mantle composition for case 68–28-Ref. with a 800 km radius impact occurring at 150 Ma with a conversion parameter of 0.6 and a velocity of 36 km/s. Atmosphere coupling is taken into account.

Impacts favor early melting, which depletes the upper mantle efficiently. Later melting (and degassing) is therefore more difficult.

The first example of lasting influence is the high venusian surface temperature created by volatile release due to the impact. Depending on the conditions, this high surface temperature period lasts for several tens up to hundreds of millions of years. As the feedback between interior and the atmosphere is taken into account, such episodes directly affect the volcanic activity of the planet.

The second consequence is related to the melt produced by the impact (see Figs. 7a, 7b, and 8). Basaltic material is formed immediately at the impact location and emplaced there, forming a thicker crust. As it cools down with time and as surface temperatures decrease it will trigger several million years later downwellings of cooler material into the hot mantle. In turn this event leads to more melting and renewed volcanic activity. The timing of major volcanic events is more difficult to pinpoint, as it depends mainly on escape flux strength: they are triggered first when surface temperature decreases (mobile lid phase), and later on at the same time as the overturn events (episodic lid phase).

Typically, we observe that during the evolution subsequent to a large impact (>400 km radius) roughly half of the activity takes place at or near the impact location, with 20% close to the antipodal position and 30% distributed over the rest of the surface.

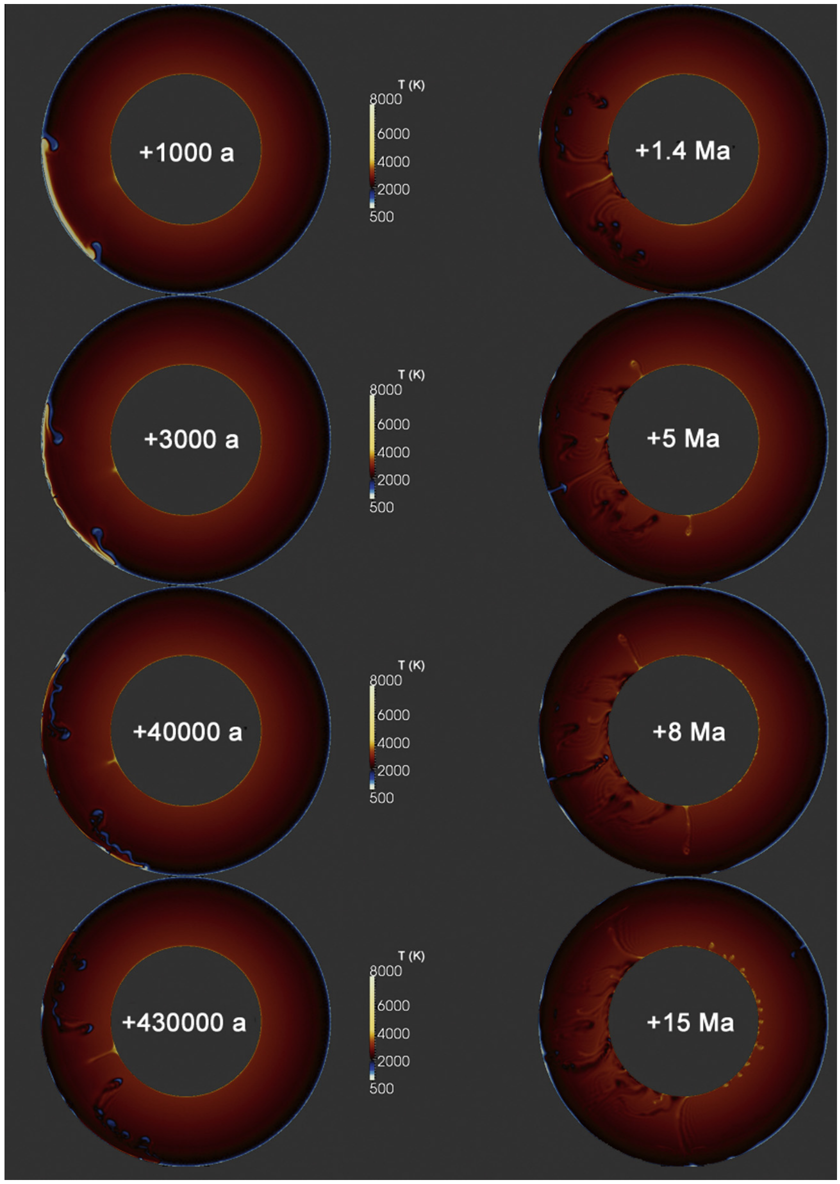

Fig. 8. Detailed evolution of venusian mantle temperatures after impact of case 68–19-Ref1 (impactor with 400 km radius hitting the planet at 150 Ma, with a conversion parameter of 0.6 and a velocity of 36 km/s), focusing on the transient upwelling occurring beneath the impact location. An antipodal downwelling can be seen in the last snapshot. Atmosphere coupling is taken into account.

These features (both antipodal and linked to the thermal anomaly) are related to the extent of the upper mantle affected by the thermal anomaly and the region where it can destabilize early crust or form new basaltic material. Three processes lead to this situation: (i) The larger impacts will completely remove early crust from most of the surface, preventing the formation of subsequent downwellings in those regions for an extended period of time. (ii) Some regions (far from the impact) are also less affected by the anomaly and exhibit thicker, colder and older crust, which will later form downwellings. (iii) Finally, melting will occur at the impact site itself, renewing the basaltic layer and causing most activity there. In the end, more basaltic material is emplaced at the impact point and near the antipodal position than at any other location on the surface of the planet.

The use of the coupled model rather than a fixed 740 K surface temperature (uncoupled) favors this repartition of activity and downwellings. Uncoupled models rarely show a specific focusing of activity at the same locations coupled models do. The coupling allows for lower surface temperatures, which tends to favor a mobile lid regime that is enhanced by these lateral differences in upper mantle structures and tends to sustain itself. As the case of large impacts (>400 km radius) occurring early on is usually associated with overall lower surface temperatures, the effect is enhanced during most of the evolution of those simulations (see Fig. 12).

Additionally, we found that the dynamics of the buoyant thermal anomaly induces large-scale movement in the upper mantle and in some cases down to the core mantle boundary. As described before, the anomaly tends to flatten and spread laterally with time as it cools down. With large anomalies, this leads to a large horizontal movement and high velocities (>10 cm/a) in the upper mantle.

An early consequence of the horizontal movement of mantle material away from the impact location is the favoring of a thermal plume from the core mantle boundary towards the upper mantle. Such events are triggered several 10^4–10^5 years after the impact

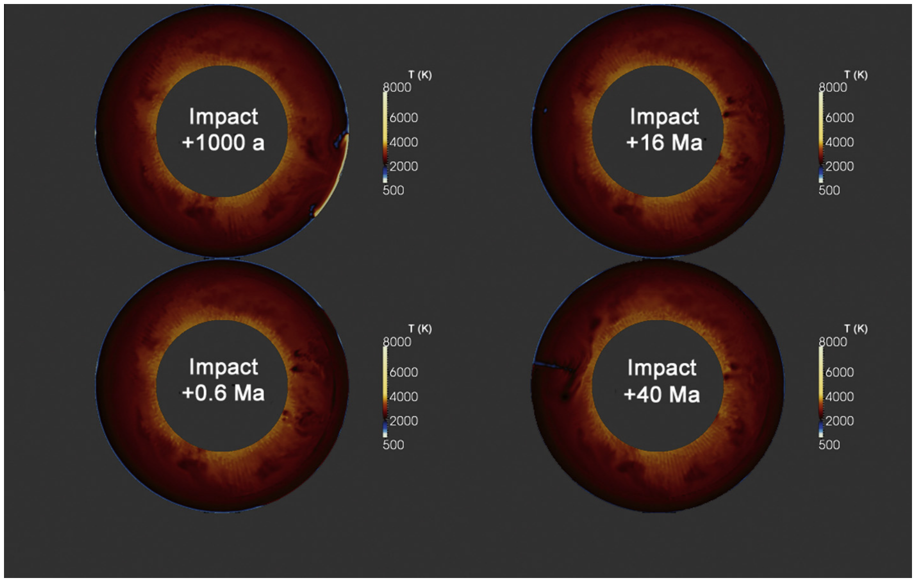

Fig. 9. Venus mantle temperature evolution after impact case 68–15-Ref-90° involving a 400 km radius impactor during the LHB epoch (at 750 Ma) with a conversion parameter of 0.6 and a velocity of 36 km/s and modified impact location. An antipodal activity spot can be observed between 16 and 40 Ma after the impact event. Atmosphere coupling is taken into account.

and last only a few million years. They are created by impactors larger than 400 km radius. This confirms the suggestion by Monteux et al. (2007) that the thermal anomaly has to penetrate the lithosphere, otherwise it diffuses away and no effect on mantle dynamics can be observed.

The same phenomenon, in conjunction with other conditions (cool surface conditions, preexistent basaltic material), seems to trigger more volcanic events during the longer-term evolution. Fig. 9 shows a common behavior after medium to large ($R_{imp} > 100$ km) impacts. It is possible to observe large-scale downwellings of colder basaltic material from the crust to the core/mantle boundary several tens to hundreds of million years after the impact occurring at the antipode of the impact location. Test simulations with different impact locations have been performed to check those events (see Table 3). The hot material spreads all over the surface, compressing the lithosphere, and due to mass conservation this forces the antipodal material to sink into the mantle. This is evidenced by the high strain-rates observed in the lithosphere in the aftermath of the impact (see Fig. 10). Depending on surface conditions (and coupling) and magnitude of the initial thermal anomaly caused by the impact, a single downwelling (opposite to the impact site) or alternatively several downwellings appear in the hemisphere opposite to the impact site. This could be dependent on the temperature/viscosity of the lithosphere and mantle since this process can be treated as a Rayleigh–Taylor instability. A colder surface, already noted to favor the mobile lid regime, seems to favor this behavior and focus the event, as does previously emplaced basaltic material that was not subducted after the impact.

3.3. Long-term effects: evolution of the planet

3.3.1. Direct effects on evolution

Regardless of the parameters used in the simulation, the basic evolution follows the same principles: melt is generated, degassing occurs, volatiles are released into the atmosphere, and surface temperature increases until those volatiles are lost to space. Variations in these parameters result in diverging regimes, with the impactor radius being the dominant parameter.

For cases with small impactors (<100 km radius), the total melt generation rate usually converges to that of the case with no impact. Testing the parameter range neither changes the results qualitatively nor adds any additional feature. The effects of the variation of those parameters on the mantle are minor. Some variation in the timing and strength of volcanic episodes can be observed, without significant consequences on the surface conditions.

For intermediate-sized impactors (100–400 km radius) it is possible to observe an intermediate situation, as low impact velocities and energy conversion parameters do not induce any response beyond the immediate consequences of the collision. However, if the chosen parameters are more extreme (meaning they enhance the thermal anomaly), they can cause the degassing of more volatiles than can be removed by atmospheric escape. At that point, they have the same effects as observed for large impactors (>400 km radius). This can lead to a permanent transition to higher surface temperatures comparable to present-day Venus conditions. In that case, the effects on the mantle results in a stagnant-lid regime, until the transition to episodic lid are reached (Gillmann and Tackley, 2014).

Volatile exchanges at impact are secondary, compared to the effects related to energy deposition into the mantle: impact erosion of the atmosphere is found to be negligible for single impacts. As observed earlier, the part of the atmosphere that can be subjected to escape is small and no more than a few percent of the atmosphere can be lost this way. This small loss of volatiles has no visible effect on the evolution of the simulations and is balanced by melt-induced degassing.

3.3.2. Long-term consequences: what makes a difference?

Major impacts lead to many modifications in the long-term evolution of Venus such as changes in mantle dynamics, melting or degassing. Most of these consequences of the impact, however, do not go beyond standard variations observed in reference models without impacts: even if they have an undeniable influence on global evolution, the same final effect could have been caused another way. Thus, our simulations indicate that impacts are not necessary to explain a particular feature of the evolution of the planet. However, there are exceptions. Interestingly enough, those exceptions

Table 3
List of simulation parameters for cases using the reference (Ref) values (see Table 1) for coupled evolution models of Venus. The same simulations were also performed with the Ref1 and Ref2 packs of parameters. "HD" indicates an additional run with higher grid resolution, "un." Indicates an additional run for an uncoupled case, "90°" indicates an additional run with modified impact location, "rhe." Indicates alternative rheology parameters (see Table 1).

Simulation name	Impactor radius (km)	Impact time (after start of simulation)	Energy conversion parameter (non-dim.)	Impactor velocity (km s^{-1})	Comment
68 Ref	0	No impact	0	0	HD, un., rhe.
68–01 Ref	50	750 Ma	0.6	20	HD; un., rhe.
68–02	50	450 Ma	0.6	36	
68–03	50	1.5 Ga	0.6	36	
68–04	50	750 Ma	0.3	20	
68–05	100	1 Ga	0.6	36	
68–06	100	750 Ma	0.9	36	
68–07	100	750 Ma	0.3	15	
68–08	100	450 Ma	0.6	36	
68–09	200	1 Ga	0.6	36	
68–10	200	750 Ma	0.3	36	
68–11	200	450 Ma	0.6	20	
68–12	200	450 Ma	0.9	36	
68–13	300	1 Ga	0.6	36	
68–14	300	450 Ma	0.9	36	
68–15	400	750 Ma	0.6	36	HD; 90°; un., rhe.
68–16	400	750 Ma	0.3	20	90°
68–17	400	450 Ma	0.6	36	
68–18	400	450 Ma	0.3	20	
68–19	400	150 Ma	0.6	36	
68–20	400	1 Ga	0.9	36	
68–21	400	1 Ga	0.6	36	
68–22	400	1 Ga	0.3	36	
68–23	400	1 Ga	0.3	46	
68–24	400	1.35 Ga	0.6	36	
68–25	400	1.75 Ga	0.6	36	
68–26	500	1 Ga	0.6	36	
68–27	500	450 Ma	0.6	36	
68–28	800	150 Ma	0.6	36	HD; 90°; un., rhe.
68–29	800	150 Ma	0.3	20	
68–30	800	150 Ma	0.9	36	
68–31	800	250 Ma	0.6	36	
68–32	800	350 Ma	0.6	36	
68–33	800	150 Ma	0.6	20	

are not related to common physical traits of large impactor. They are directly linked to the time of the impact event.

Fig. 11 illustrates the importance of timing for the long-term evolution of surface conditions. Impacts occurring at three different times are shown together with a reference case without an impact. While the present-day surface conditions are similar enough in those four cases ($\sim$25 K difference in surface temperature among the cases), the evolution of the models leading to the present-day state is very different. Two simulations (no impact or exceptionally late large impact) experience a low surface temperature period between 3.5 and 3 Ga ago. As shown previously, this triggers plate-like behavior. The other two cases (LHB impact or impact at 3.5 Ga ago) completely bypass that period by releasing sufficient amounts of volatiles into the atmosphere. Thus surface temperature stays high and stagnant lid/episodic lid occurs throughout the entire planetary evolution.

A second example shown in Fig. 12 focuses on the LV era. We can observe that the evolution of surface conditions is completely modified by the occurrence of a major impact early on. Indeed, the late evolution is marked by surface temperature reduction by 60–100 K for the case including an impact. Looking into more detail, we see that the "low temperature era" common to those simulations starts a few tens to a hundred Ma later than in cases without an impact event. It also extends for 500 Ma longer until 2.5–2 Ga ago instead of 3–2.8 Ga. During that era, fewer spikes of higher surface temperatures can be observed. Even after temperatures have risen again, the rate of increase is small and values stay lower than in models featuring an impact. Melt production (volcanic activity) shows that the early evolution of the impact case is dominated by melt produced by the impact itself.

Following the impact, small amounts of melt are produced for 500 Ma and then large-scale volcanic activity occurs again for the next 2 Ga. Later activity is low but continuous. The reference case (no impact) behaves differently (see Gillmann and Tackley, 2014), with some early activity, a large spike after 4 Ga and afterwards more sporadic vigorous activity in the form of spikes separated by quiescent periods. In short, the impact seems to concentrate most of the high activity into the era between 4 and 3 Ga ago, whereas the case without impact displays spikes of activity throughout most of the planet's history.

Mean mantle temperatures also show differences between these two cases. While the same early increase in mean mantle temperature is observed in the model without an impact, it is more pronounced in the case where an impact occurs since the lack of post-impact volcanism does not allow for efficient heat removal. It results in more intense volcanism when the lid is broken at 4–3 Ga ago. The absence of early volcanism after the impact can be attributed to the disruption of early mantle plumes by the impactor and the large scale melting of the upper mantle that leads to its substantial depletion while forming a large amount of basaltic crust. This layer would only destabilize later on, when surface temperatures decrease. The late mean temperature evolution shows an effective cooling of the mantle.

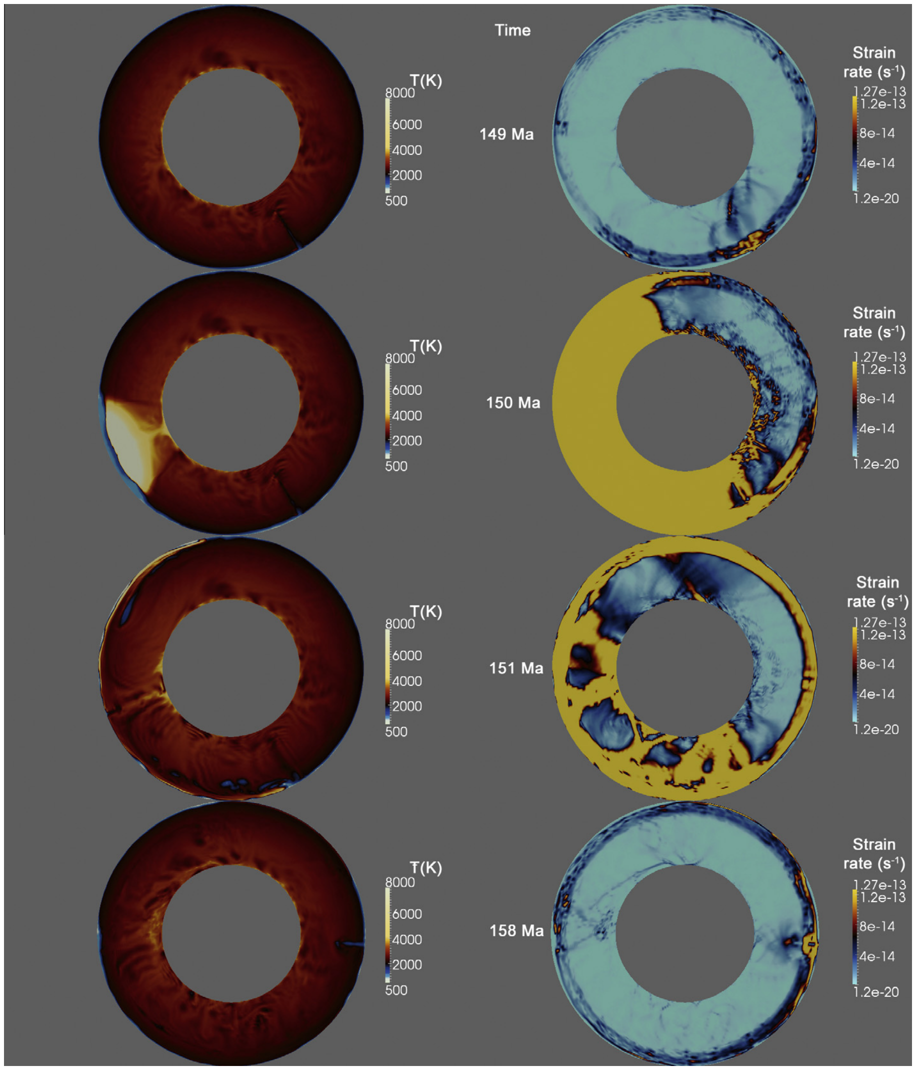

Fig. 10. Short-term evolution of venusian mantle temperature and mantle strain-rate for case 68–28-Ref. with a 800 km radius impact occurring at 150 Ma with a conversion parameter of 0.6 and a velocity of 36 km/s. For the sake of visibility, the strain-rate range has been cut-off at values relevant for the pre-impact situation, thus explaining the saturation of the field at and immediately after the impact. Atmosphere coupling is taken into account.

Without an impact, the mantle temperature reaches early on lower values, translating into less intense, but more spread-out volcanism. The major temperature increase occurs later, when the surface temperature rises again, thus resulting in a stagnant lid regime, insulating the mantle. On the contrary, in the impact case the surface temperature never rises considerably during the late evolution, thus no stagnant lid forms and heat is lost more efficiently.

In summary, the impact leads to massive degassing and depletion of the mantle very early on by (i) directly melting a large portion of the upper mantle and (ii) enhancing early volcanic activity (during the era 4–3 Ga ago). The consequences are a depleted upper mantle that is more difficult to melt later on and a major loss of volatiles early on, when they are efficiently lost to space. In contrast, the simulation without an impact releases volatiles later on, over an extended period of time, with late spikes of activity ensuring replenishment of water in the atmosphere.

4. Discussion

Our results clearly show that while single major impacts can strongly affect the surface conditions of a planet, all mechanisms involved do not have lasting effects on its long-term evolution. For clear, large-scale consequences, the impact must exhibit a rather peculiar set of parameters, including timing. Otherwise, only local or short-term effects will usually be observed. In the end, direct volatile exchanges are not as important as the energy deposition.

Recent studies (Shuvalov, 2009, 2010; Shuvalov et al., 2014) on impact erosion led to estimations that single impacts could only remove a small fraction of a terrestrial planet's atmosphere. Based on those estimates, it appears that this process is insufficient to have a significant effect on the long-term evolution. It is actually completely offset by other effects involved that lead to degassing of volatiles and replenishment of the atmosphere. Still, it could lead to interesting effects on a planetary body other than Venus, for example on Titan (Zahnle et al., 1992; Marounina et al., 2014), or Mars (Vickery, 1990; Pham et al., 2011; Maindl et al., 2014). Venus' thick atmosphere does not experience significant impact-induced changes, because of the already large CO_2 pressure. Small water concentration changes can affect the surface temperature, but at this level it amounts to roughly what can be released by a volcanic event and is by no means uncommon. Additionally, the other two effects (melting and volatiles from the

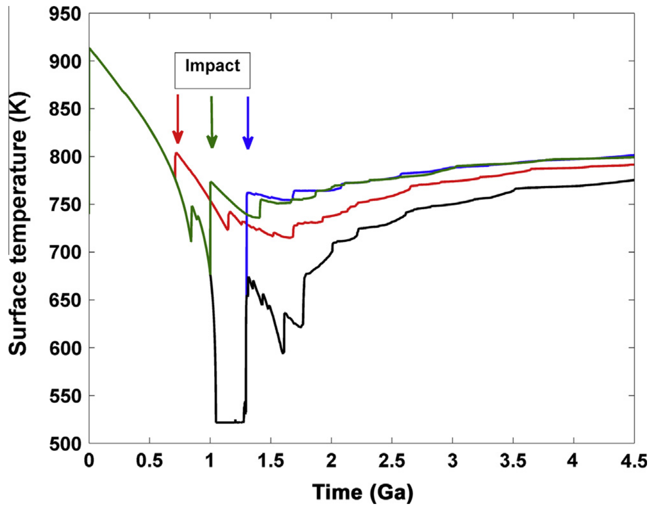

Fig. 11. Long-term surface temperature evolution with time for four different cases: no impact (black), impact at 3.8 Ga (red), impact at 3.5 Ga (green), impact at 3.2 Ga (blue). All impactors have 400 km radius. (For interpretation of the references to color in this figure legend, the reader is referred to the web version of this article.)

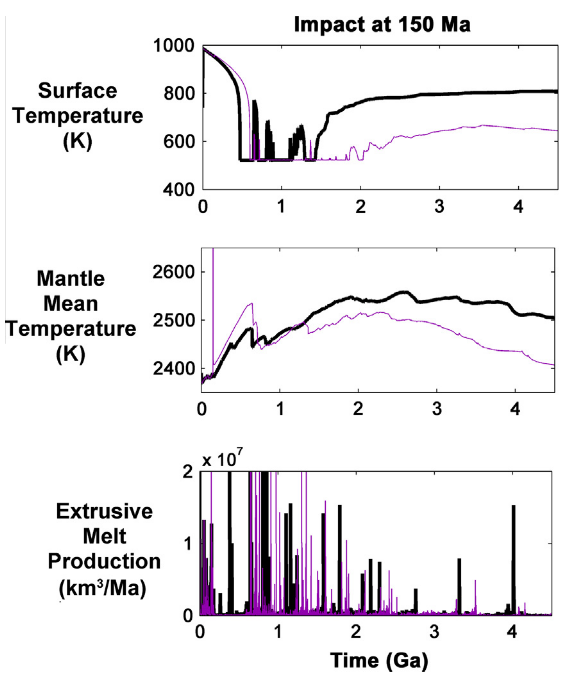

Fig. 12. Comparison between the evolution of a reference case (black) without impact and a LV impact (purple) occurring 4.4 Ga ago with a 800 km radius impactor. Surface temperature evolution, mean mantle temperature and extrusive melt production rate are plotted. (For interpretation of the references to color in this figure legend, the reader is referred to the web version of this article.)

impactor) directly counteract erosion on a short timescale. We attribute this to the single giant impact scenario we use. Indeed, numerous smaller impacts may have a different effect (Schlichting et al., 2015), a scenario we will test in the future.

Volatile input from the impactor is also not considered in the present simulations, but would probably not add qualitative features to the simulations, while the amount of volatiles (mainly water) brought by impactors has been stated to be significant, especially during the accretion but also afterwards (Zahnle et al., 1988; Hamano et al., 2013; Segura et al., 2013). In the case of an 800 km chondritic impactor with a water concentration in the 0.1–3% range, around $5\text{–}150 \times 10^{18}$ kg of water can be delivered. Conventional scaling (Cintala and Grieve, 1994) implies that for the velocities used in our simulations, the immediate melt mass is around thirty times the mass of the impactor. This would mean the release of around $1\text{–}40 \times 10^{18}$ kg of water from the melt only, depending on the composition of Venus' mantle. Considering a large impactor, melting is, in our models, not restricted to the crater formation phase and can reach up to four times the amount mentioned. Therefore, the amounts of water released by the impactor itself and melting of the target body are comparable. Delivery by the impactor can even be the main water source in cases where volatile-rich chondritic material impacts an already degassed Venus with a dry mantle.

It is also still unclear how material constituting the impactor is distributed after the impact, especially for large events (O'Neill and Palme, 2008; Rivera-Valentin and Barr, 2014; Kraus et al., 2015): How is it incorporated into the planet? What part is vaporized? How does it mix into the mantle? Those mechanisms would make it worth considering the impactor as a volatile source rather than just adding a more or less constrained amount of gases into the atmosphere of the planet during the impact. In the face of those additional uncertainties, we postpone the inclusion of these effects to future work, after assessing the consequences of the other mechanisms.

Although we observed that large impacts could lead to the appearance of a plume from the core mantle boundary beneath the impact location, it does not appear to be the focused long-term feature observed by other studies that tried to reproduce martian features like the crustal dichotomy and the Tharsis volcanic province by means of impacts. In our case, after the thermal anomaly has spread we only observe a transient plume. For the case of Mars Golabek et al. (2011) and Reese et al. (2004, 2010) describe the formation of a transient superplume caused by shear heating during the sinking of the impactor core and later on an aggregation of multiple plumes over the evolution of the planet and their stabilization in one single stable upwelling of hot material in a fixed location. Other differences in behavior are probably due to the different size and rheology of these two planets (van Thienen et al., 2004). Future simulations covering a wider range of rheologies will help to assess this.

On the other hand, we observe large-scale downwellings following large impacts, in which basaltic crustal material sinks roughly at the antipode of the impact location on a timescale of millions of years. Our simulations suggest that this mechanism is favored by lower surface temperatures causing a transition from stagnant lid to mobile lid regime. It has long been suggested that major volcanic events could be a consequence of an antipodal impact (Ronca, 1966; Rampino, 1987; Nimmo et al., 2008; Meschede et al., 2011). The usual mechanism invoked to explain this possibility is the convergence of seismic waves at the antipode of the impact site (Boslough et al., 1995). This theory has detractors (Melosh, 2000), who view the energy produced at the antipode as too small to trigger any substantial event and add that a main "evidence" for this mechanism (the Chicxulub–Deccan traps link) has been disproved (Bhandari et al., 1995). While we observe antipodal melting linked to the impact in our model, it is not by the process described above. First, the considered impactors are more than one order of magnitude larger than the Chicxulub meteorite. Secondly, the melting does not always occur precisely at the antipodal position as would be expected from the focusing of seismic waves for a head-on impact (Marinova et al., 2011). Instead, it is linked to the downwelling of basaltic crustal material. We show that for a sufficiently large thermal anomaly, such as is generated by a fast large impact, upper mantle horizontal velocities are the origin of the activity. Anomaly spreading and melt emplacement on top of the mantle control the lateral displacement discussed earlier. The spreading of hot material at the surface forces the antipodal crust to sink due to conservation of mass. This is enhanced by the fact that antipodal material is usually the oldest crust remaining after large impacts. However, this mechanism does not result in stable plumes on the long-term, but only causes a single event. Thus, rather than a sustained feature like a long-lived plume triggered by the impact, we observe a succession of events each paving the way to the next.

Our simulations put the emphasis on single large impacts. We consider the largest possible impactors that can be expected for the studied periods of time (LV and LHB), by concentrating most of the total impacting mass into a single impact as suggested for the LV phase (Bottke et al., 2010; Raymond et al., 2013). The point was to test what kind of impacts can have lasting consequences, and it appears, impactors need to be large (>400 km radius) to have permanent, global effects. Still, objects with 100–400 km radius can affect the planet and its mantle, albeit not as drastically. Our results suggest that single impactors with 50–100 km radius are probably not large enough to have more than a local and short-term effect, a conclusion also found by Roberts and Barnouin (2012) for the case of Mercury.

In a more realistic approach – one that we will implement in the next stage of our work – a successive impact history should be considered (e.g. the Venus data from Raymond et al. (2013)). Selecting the largest impacts possible introduces a bias toward one effect compared to others. Each population of bodies would favor a specific mechanism. At the present level of knowledge, given how inefficient impact erosion seems to be (Shuvalov, 2009, 2010; Shuvalov et al., 2014) and how it scales with size, a multitude of small impacts may have a more pronounced effect than a single impact as suggested by several studies (Pham et al., 2009; Pham, 2012; Schlichting et al., 2015). For the same reasons, volatile delivery needs to be studied using a realistic impact history. However, it must be noted that realistic simulations for large impacts are sorely needed and that modeling work done at present-day deals at most with bodies smaller than 100 km diameter. Larger impactors lead to additional difficulties and mechanisms we need to understand to properly define their role in the evolution of terrestrial planets.

4.1. Model limitations

As it is the case with all models, the one explored in this work suffers from some limitations. Some were already discussed in Gillmann and Tackley (2014) and we will focus on how they affect the impact simulations.

First, the modeling of impacts and their effects is simplified. We neglect the case of oblique impacts in order to focus on head-on events. The angle of impact can have an influence on erosion efficiency, as shown by Shuvalov (2009, 2010), by enhancing the process. This implies that in those cases, our erosion calculations are only a lower limit. Variation of erosion induced by the impact angle would fall inside the error bar induced by the extrapolation to larger bodies. In the end, the main effect of the angle of impact would probably be the mixing of material: one can imagine that a head-on impact could lead to a rapid merger of the two metallic cores while a oblique collision could lead to more mixing of material, adding much complexity since the iron core could break up during collision (Kraus et al., 2015). A part of the impactor and of the impacted planet should be redistributed over the surface of the target body (Maxwell, 1977), creating a high temperature layer. Such a layer would have effects on the surface conditions of the planet. However, it is most likely that those effects would be short-lived since cooling of such a layer would be fast compared to the timescale of global convection.

Not taken into account are mostly processes related to the solid part of the impactor. We have also neglected the processes linked to the excavation of a crater. However it is likely that this is of little consequence since most of the energy is stored below the crater (Turtle et al., 2003). During the isostatic relaxation process, a vertical motion of a few kilometers occurs on the order of 10^3 years (Monteux et al., 2007). Thermal readjustment of the thermal anomaly is therefore the dominant process on the long-term and global scale.

Atmosphere erosion processes are also less than perfectly constrained. Our approach relies on modeling efforts using the SOVA code (Shuvalov, 1999). However, most of the available studies focus on small impacts. The accepted conclusion is that those single impacts do not remove a significant part of the planetary atmosphere (de Niem et al., 2012). For larger collision events, we can only extrapolate these results, which are less than ideal but still fits with other simple calculations like the tangent plane model. Further modeling is needed to assess whether larger impacts' eroding power is in line with the cases studied until now. The main problem is that the sizes of large impactors are comparable to the atmosphere thickness of the target planets, requiring more computational power to perform the simulations.

Another limitation is the problem of the timescales. As already mentioned, impacts are punctual events that have consequences on all timescales from a second to billions of years. We are not able to use time steps that would allow us to calculate atmospheric effects and mantle convection at the same time. The mantle convection code is limited to time steps longer than 10^4 years. Some effects of the impacts (surface ocean evaporation, silicate vapor, etc.) last less than 10^3 years after an impact (Zahnle et al., 2007; Lupu et al., 2014), thus cannot be modeled in our simulations. Additionally, those transient surface conditions modifications are likely to have a small effect on the long-term evolution of the planet.

On the other hand, at present we do not use an atmosphere model that is able to realistically take into account those short-term events and adapt to the widely different surface and atmospheric conditions that emerge in the aftermath of an impact. The atmosphere code we use is based on Venus' present-day conditions and allows for moderate variations around that starting point. Also, evolution of the atmosphere chemistry is not taken into account. For example, it would become unreliable in cases where large amounts of water are brought into the atmosphere of Venus or if the background CO_2 atmosphere was lost. A reason for that is the presence of clouds. In the model we assume present-day clouds. For example it is currently uncertain how the cloud layer would react to the presence of large amounts of water (Bullock and Grinspoon, 2001). They could disappear, completely changing surface conditions, resulting in a much higher surface temperature. In this way, given the present state of our knowledge and the current model, it is best not to include those short-term processes in the simulations.

Concerning the convection part of the model, it is important to remember that only the 2D spherical annulus geometry has been studied at present. It is possible that compared to a full 3D geometry, the 2D spherical annulus overestimates the degassing by a margin. This can be explained by the fact that the ratio of the affected volume of mantle (proportional to R_{ic}) to the total mantle volume (proportional to R) is larger in the 2D case (the R_{ic}/R ratio is squared) than in 3D geometry (the ratio is cubed). Later work will employ 3D calculations to assess the effect of this change in geometry on the long-term evolution. In the current code, the local magma ocean produced at the impact location is treated in a simplified way. Only the basaltic component of the mantle is allowed to melt while the temperatures reached would permit the melting of the whole solid phase for a short time. Additionally, the lower viscosity cut-off can affect the behavior of the magma ocean and the speed of its evolution. Golabek et al. (2011) noted that it could limit the spreading of such an impact-related magma ocean.

Finally, due to the number of parameters involved, we did not vary the solid planet parameters in this study beyond simple volatile concentration changes. We kept the reference case rheological parameters from Gillmann and Tackley (2014) (see Table 1) (e.g. viscosity profile, reference viscosity, plastic yielding, reference yield stress, initial temperature). Changes in the rheology of the planet would have a direct effect on the exact response of the simulations to the large impact. While the immediate consequences (initial melting, degassing, surface temperature increase) would not be affected, and some responses would probably not vary significantly (thermal anomaly spreading), the long-term evolution could be somewhat different. Near crustal processes might be significantly affected, as may be the location, strength and duration of mantle plumes. Recent work (Tackley, 2015) has highlighted the importance of the emplacement of melt when it is extracted from the mantle. This work indicates that episodic activity on Venus can occur without requiring a plastic rheology when part of the melt intrudes the crust, causing a weak crust, instead of assuming a completely extrusive crust formation. Also, interaction between gases and the hot rocks and magma, which may affect the surface conditions, is neglected. Adding this to the model will require a better estimation of melt propagation to the surface and the inclusion of long-term geochemical evolution into the model.

4.2. Evolution of Venus and possible early habitability

The effects of the studied impacts would not be obvious from observations of the present-day atmosphere: cases that include impacts are not clearly distinct from cases without impacts. The total CO_2 amount in the atmosphere could differ. Comparison of present-day CO_2 partial pressure in the atmosphere of Venus to a hypothetic evolution where no impact occurred could theoretically allow us to quantify the number (or at least total mass) of impactors. However, this is not practical due to the lack of constraints on key parameters for volatile evolution (volatile concentrations in the mantle, efficiency of degassing, geological history dating back to more than 300–1000 Ma). Without a precise volcanic history, reconstruction of the degassing throughout the evolution of the planet is not possible. Impacts are also unlikely to generate a significant and measurable isotopic fractionation by eroding the atmosphere. However, considering the results highlighted by this work, they could have a significant effect on the mantle state and convection (such as a lower present-day mean temperature in the cases where a large impact occurred). Markers for those modifications are not obvious either and would not appear on the young surface, which makes it even more important to assess if older surface rocks could be found somewhere on Venus. Older buried material is also out of reach for now, but could provide valuable data.

Large LV impacts seem to be able to deplete Venus' volatile inventory and upper mantle efficiently. Simulations including this type of scenario are unlikely to end close to the present-day observed state. However, it is also very likely that Venus experienced at least one of those impacts during its early history (Raymond et al., 2013). For Venus to behave as it does, more water is needed, either by not degassing its mantle early on, or by replenishing it during/after those large impacts.

Regarding the habitability problem, it is unlikely that a single giant impact could be responsible for the emergence of favorable conditions. A hypothesis states that erosion by such a collision could have facilitated the occurrence of a window of low surface temperature (Lenardic et al., 2008; Gillmann and Tackley, 2014) that could enable subduction and CO_2 sequestration (Driscoll and Bercovici, 2013), in the presence of water (e.g. McGovern and Schubert, 1989; Nimmo and McKenzie, 1998; Korenaga, 2010). It appears that erosion is not sufficient to affect surface conditions significantly. Actually, the degassing of volatiles and in particular of CO_2 (which is moderate when only volcanism is considered over the whole 4.5 Ga) is considerably enhanced and leads to the opposite effect. Atmospheric erosion would need to be orders of magnitude more efficient to support this hypothesis. Additionally, the easiest way to lower the surface temperature is to remove the already scarce water from the atmosphere. This leads to surface temperatures in the range of 500–600 K, but obviously prevents the condensation of water. Indeed some impact scenarios result in lower surface temperatures precisely because water is absent in the atmosphere due to massive early degassing and loss.

5. Conclusions

We have studied the influence of a single large impact on the long-term evolution of Venus and its surface conditions and our main conclusions are

(1) For single impact models, both atmospheric erosion and volatile delivery by the impactor have minor effects on the long-term evolution of the planet. Melt generation is the dominant process.
(2) Only impactors with >400 km radius and high energy collisions (high velocity/energy deposition parameter) have lasting effects on the evolution of the planet through volatile degassing and energy deposition in the mantle. Smaller collisions have local consequences only.
(3) Large impacts tend to focus later volcanic activity and downwellings in specific locations: near the impact location and around the antipodal position.
(4) Early collisions (LV case), occurring at a time when atmospheric escape is intense, can lead to the efficient depletion of the mantle and remove water from the planet early on.
(5) Later collisions (LHB case) occur when atmospheric escape has diminished considerably. In such cases, the atmosphere is wetter than present-day Venus and surface temperature stays stable and high. This has implications for mantle dynamics through atmosphere/mantle coupling.
(6) Based on these simulations, the role of large impacts on the evolution of Venus cannot yet be distinguished by its present climate. However, we have proposed several impact evolution pathways that can account for the present-day state of Venus.

Acknowledgments

We thank Francis Nimmo for helpful discussions on the process of atmosphere erosion, Martina Ulvrová for her help with the strain-rate plots and Philippe Lognonné for his role in the origins of this project. This work was performed at the Royal Observatory of Belgium, as part of Planet TOPERS, with funding by the Interuniversity Attraction Pole Program initiated by the Belgian Science Policy Office. We also thank Kevin Zahnle and an anonymous reviewer for their insightful reviews, which helped to improve the manuscript.

Appendix A. Supplementary material

Supplementary data associated with this article can be found, in the online version, at http://dx.doi.org/10.1016/j.icarus.2015.12.024.

References

Abramov, O., Mojzsis, S.J., 2009. Microbial habitability of the Hadean Earth during the Late Heavy Bombardment. Nature 459, 419–422.

Ahrens, T.J., 1993. Impact erosion of terrestrial planetary atmospheres. Ann. Rev. Earth Planet. Sci. 21, 525–555.

Armann, M., Tackley, P.J., 2012. Simulating the thermochemical magmatic and tectonic evolution of Venus's mantle and lithosphere: Two-dimensional models. J. Geophys. Res. 117. http://dx.doi.org/10.1029/2012JE004231 E12003.

Baines, K.H. et al., 2013. The atmospheres of the terrestrial planets: Clues to the origins and early evolution of Venus, Earth, and Mars. In: Mackwell, S.J. et al. (Eds.), Comparative Climatology of Terrestrial Planets. Univ. of Arizona, Tucson, pp. 137–160.

Bauer, S.J., Lammer, H., 2004. Planetary Aeronomy: Atmosphere Environments in Planetary Atmospheres. Springer, Berlin, Heidelberg, New York, p. 207.

Bercovici, D., Lin, J., 1996. A gravity current model of cooling mantle plume heads with temperature-dependent buoyancy and viscosity. J. Geophys. Res. 101, 3291–3310.

Bhandari, N. et al., 1995. Impact did not trigger Deccan volcanism: Evidence from Anjar K/T Boundary intertrappean sediments. Geophys. Res. Lett. 22, 433–436.

Boslough, M.B. et al., 1995. Axial focusing of energy from a hypervelocity impact on Earth. Int. J. Impact Eng. 17, 99–108.

Bottke, W.F. et al., 2007. Can planetesimals left over from terrestrial planet formation produce the lunar Late Heavy Bombardment? Icarus 190, 203–223.

Bottke, W.F. et al., 2010. Stochastic late accretion to Earth, the Moon, and Mars. Science 330, 1527–1530.

Bottke, W.F. et al., 2012. An Archaean heavy bombardment from a destabilized extension of the asteroid belt. Nature 485, 78–81.

Britt, D.T. et al., 2002. Asteroid density, porosity and structure. In: Bottke, W.F., Cellino, A., Paolicchi, P., Binzel, R.P. (Eds.), Asteroids III. Univ. of Arizona Press, Tucson, pp. 485–500.

Bullock, M.A., Grinspoon, D.H., 1996. The stability of climate on Venus. J. Geophys. Res. 101, 7521–7529.

Bullock, M.A., Grinspoon, D.H., 2001. The recent evolution of climate on Venus. Icarus 150, 19–37.

Cameron, A.G.W., 1983. Origin of the atmospheres of the terrestrial planets. Icarus 56, 195–201.

Cameron, A.G.W., Ward, W.R., 1976. The origin of the Moon. Lunar Planet. Sci. Conf. vol. 7. Abstracts 120.

Canup, R.M., 2004. Simulations of a late lunar-forming impact. Icarus 168, 433–456.

Canup, R.M., 2012. Forming a Moon with an Earth-like composition via a Giant Impact. Science 338, 1052–1055.

Canup, R.M., Asphaug, E., 2001. Origin of the Moon in a giant impact near the end of the Earth's formation. Nature 412, 708–712.

Chassefière, E., 1996a. Hydrodynamic escape of oxygen from primitive atmospheres: Applications to the cases of Venus and Mars. Icarus 124, 537–552.

Chassefière, E., 1996b. Hydrodynamic escape of hydrogen from a hot water-rich atmosphere: The case of Venus. J. Geophys. Res. 101, 26039–26056.

Chassefière, E., Leblanc, F., 2004. Mars atmospheric escape and evolution: Interaction with the solar wind. Planet. Space Sci. 52, 1039–1058.

Chen, G.Q., Ahrens, T.J., 1997. Erosion of terrestrial planet atmosphere by surface motion after a large impact. Phys. Earth Planet. Int. 100, 21–26.

Cintala, M.J., Grieve, R.A.F., 1994. The effects of differential scaling of impact melt and crater dimensions on lunar and terrestrial craters: Some brief examples. Spec. Pap. Geol. Soc. Am. 293, 51–60.

Crisp, J.A., 1984. Rates of magma emplacement and volcanic output. J. Volc. Geotherm. Res. 20, 177–211.

Croft, S.K., 1982. A first order estimate of shock heating and vaporization in oceanic impacts. In: Silver, T.L., Schultz, P.H. (Eds.), Geological Implications of Impacts of Large Asteroids and Comets on Earth, Special Papers, vol. 190. Geol. Soc. Am., pp. 143–152.

Dauphas, N., 2003. The dual origin of the terrestrial atmosphere. Icarus 165, 326–339.

de Niem, D. et al., 2012. Atmospheric erosion and replenishment induced by impacts upon the Earth and Mars during a heavy bombardment. Icarus 221, 495–507.

Driscoll, P., Bercovici, D., 2013. Divergent evolution of Earth and Venus: Influence of degassing, tectonics, and magnetic fields. Icarus 226, 1447–1464.

Elkins-Tanton, L.T. et al., 2007. Volcanism and volatile recycling on a one-plate planet: Applications to Venus. J. Geophys. Res. 112 E04S06.

Frey, H., 2008. Ages of very large impact basins on Mars: Implications for the heavy bombardment in the inner Solar System. Geophys. Res. Lett. 35 L13203.

Genda, H., Abe, Y., 2003. Survival of a proto-atmosphere through the stage of giant impacts: The mechanical aspects. Icarus 164, 149–162.

Gillmann, C., Chassefière, E., Lognonné, P., 2009. A consistent picture of early hydrodynamic escape of Venus atmosphere explaining present Ne and Ar isotopic ratios and low oxygen atmospheric content. Earth Planet. Sci. Lett. 286, 503–513.

Gillmann, C., Tackley, P.J., 2014. Atmosphere/mantle coupling and feedback on Venus. J. Geophys. Res. 119, 1189–1217.

Golabek, G.J. et al., 2011. Origin of the martian dichotomy and Tharsis from a giant impact causing massive magmatism. Icarus 215, 346–357.

Gomes, R. et al., 2005. Origin of the cataclysmic Late Heavy Bombardment period of the terrestrial planets. Nature 435, 466–469.

Gough, D.O., 1981. Solar interior structure and luminosity variations. Solar Phys. 74, 21–34.

Grinspoon, D.H., 1993. Implications of the high D/H ratio for the sources of water in Venus' atmosphere. Nature 363, 428–431.

Hamano, K., Abe, Y., 2010. Atmospheric loss and supply by an impact-induced vapor cloud: its dependence on atmospheric pressure on a planet. Earth Planets Space 62, 599–610.

Hamano, K., Abe, Y., Genda, H., 2013. Emergence of two types of terrestrial planet on solidification of Magma Ocean. Nature 497, 607–611.

Hartmann, W.K., Davis, D.R., 1975. Satellite-sized planetesimals and lunar origin. Icarus 24, 504–515.

Hernlund, J.W., Tackley, P.J., 2008. Modeling mantle convection in the spherical annulus. Phys. Earth Planet. Int. 171, 48–54.

Herrick, R.R., 1994. Resurfacing history of Venus. Geology 22, 703–706.

Hunten, D., Pepin, R.O., Walker, J., 1987. Mass fractionation in hydrodynamic escape (of gases from planetary atmospheres). Icarus 69, 532–549.

Ivanov, B.A., 2001. Mars/Moon cratering rate ratio estimates. Space Sci. Rev. 96, 87–104.

Jacobson, S.A. et al., 2014. Highly siderophile elements in Earth's mantle as a clock for the Moon-forming impact. Nature 508, 84–87.

Jakosky, B.M. et al., 1994. Mars atmospheric loss and isotopic fractionation by solar-wind induced sputtering and photochemical escape. Icarus 111, 271–288.

Janle, P. et al., 1992. Heat-loss and tectonic style of Venus. Earth Moon Planets 58, 1–29.

Jørgensen, U.G. et al., 2009. The Earth–Moon system during the Late Heavy Bombardment period – Geochemical support for impacts dominated by comets. Icarus 204, 368–380.

Karato, S., Wu, P., 1993. Rheology of the upper mantle – A synthesis. Science 260, 771–778.

Kasting, J.F., Catling, D., 2003. Evolution of a habitable planet. Ann. Rev. Astron. Astrophys. 41, 429–463.

Kasting, J.F., Pollack, J.B., 1983. Loss of water from Venus. I. Hydrodynamic escape of hydrogen. Icarus 53, 479–508.

Kasting, J.F., Pollack, J.B., Ackerman, T.P., 1984. Response of Earth's atmosphere to increases in solar flux and implications for loss of water from Venus. Icarus 57, 335–355.

Koch, D.M., Manga, M., 1996. Neutrally buoyant diapirs: A model for Venus Coronae. Geophys. Res. Lett. 23, 225–228.

Kraus, R.G. et al., 2015. Impact vaporization of planetesimal cores in the late stages of planet formation. Nat. Geosci. 8, 269–272.

Korenaga, J., 2010. On the likelihood of plate tectonics on super-Earths: Does size matter? Astrophys. J. Lett. 725, 43–46.

Lammer, H. et al., 2003a. Loss of water from Mars: Implications for the oxidation of the soil. Icarus 106, 9–25.

Lammer, H. et al., 2003b. Atmospheric loss of exoplanets resulting from stellar X-ray and extreme ultraviolet heating. Astrophys. J. 598, L121–L124.

Lenardic, A., Jellinek, A.M., Moresi, L.-N., 2008. A climate induced transition in the tectonic style of a terrestrial planet. Earth Planet. Sci. Lett. 271, 34–42.

Levison, H.F. et al., 2001. Could the lunar "Late Heavy Bombardment" have been triggered by the formation of Uranus and Neptune? Icarus 151, 286–306.

Levison, H.F. et al., 2011. Late orbital instabilities in the outer planets induced by interaction with a self-gravitating planetesimal disk. Astronom. J. 142, 142–152.

Lundin, R., Barabash, S., 2004. Evolution of the martian atmosphere and hydrosphere: Solar wind erosion studied by ASPERA-3 on Mars Express. Planet. Space Sci. 52, 1059–1071.

Lupu, R.E. et al., 2014. The atmospheres of Earth-like planets after giant impact events. Astrophys. J. 784, 784-27 (19pp).

Maindl, T.I., Dvorak, R., Schäfer, C., Speith, R., 2014. Fragmentation of colliding planetesimals with water content. In: Proceedings of the International Astronomical Union 9, Symposium, S310.

Marinova, M.M., Aharonson, O., Asphaug, E., 2011. Geophysical consequences of planetary-scale impacts into a Mars-like planet. Icarus 211, 960–985.

Marounina, N. et al., 2014. Evolution of Titan's atmosphere during the Late Heavy Bombardment. Icarus 257, 324–335.

Marty, B., Meibom, A., 2007. Noble gas signature of the Late Heavy Bombardment on the Earth's atmosphere. eEarth 2, 43–49.

Maxwell, D.E., 1977. Simple Z model for cratering, ejection and the overturned flap. In: Roddy, D.J., Pepin, R.O., Merrill, R.B. (Eds.), Impact and Explosion Cratering: Planetary and Terrestrial Implications. Elsevier, New York, pp. 1003–1008.

McGovern, P.J., Schubert, G., 1989. Thermal evolution of the Earth: Effects of volatile exchange between atmosphere and interior. Earth Planet. Sci. Lett. 96, 27–37.

McKenzie, D., Bickle, M.J., 1988. The volume and composition of melt generated by extension of the lithosphere. J. Petrol. 29 (3), 625–679.

McKinnon, W.B. et al., 1997. Cratering on Venus: Models and observations. In: Bougher, Stephen W., Hunten, D.M., Philips, R.J. (Eds.), Venus II. Arizona Univ. Press, pp. 969–1014.

Melosh, H.J., 2000. Can impacts induce volcanic eruptions? In: International Conference on Catastrophic Events and Mass Extinctions: Impacts and Beyond. Abstract no. 3144.

Melosh, H.J., Vickery, A.M., 1989. Impact erosion of the primordial atmosphere of Mars. Nature 338, 487–489.

Meschede, M.A., Myhrvold, C.L., Tromp, J., 2011. Antipodal focusing of seismic waves due to large meteorite impacts on Earth. Geophys. J. Int. 187, 529–537.

Monteux, J. et al., 2007. Thermo-mechanical adjustment after impacts during planetary growth. Geophys. Res. Lett. 34 L24201.

Nakagawa, T., Tackley, P.J., 2004. Effects of thermo-chemical mantle convection on the thermal evolution of the Earth's core. Earth Planet. Sci. Lett. 220, 107–119.
Nakagawa, T., Tackley, P.J., 2005. The interaction between the post-perovskite phase change and a thermo-chemical boundary layer near the core–mantle boundary. Earth Planet. Sci. Lett. 238, 204–216.
Nakagawa, T., Tackley, P.J., 2010. Influence of initial CMB temperature and other parameters on the thermal evolution of Earth's core resulting from thermo-chemical spherical mantle convection. Geophys. Geochem. Geosyst. 11. http://dx.doi.org/10.1029/2010GC003031 Q06001.
Nakagawa, T. et al., 2009. Incorporating self-consistently calculated mineral physics into thermo-chemical mantle convection simulations in a 3D spherical shell and its influence on seismic anomalies in Earth's mantle. Geochem. Geophys. Geosyst. 10. http://dx.doi.org/10.1029/2008GC002280 Q03004.
Nakagawa, T. et al., 2010. The influence of MORB and harzburgite composition on thermo-chemical mantle convection in a 3-D spherical shell with self-consistently calculated mineral physics. Earth Planet. Sci. Lett. 296, 403–412.
Namiki, N., Solomon, S.C., 1998. Volcanic degassing of argon and helium and the history of crustal production on Venus. J. Geophys. Res. 103, 3655–3678.
Newman, W.I. et al., 1999. Impact erosion of planetary atmospheres: Some surprising results. Icarus 138, 224–240.
Nimmo, F., McKenzie, D.P., 1997. Convective thermal evolution of the upper mantles of Earth and Venus. Geophys. Res. Lett. 24, 1539–1543.
Nimmo, F., McKenzie, D., 1998. Volcanism and tectonics on Venus. Ann. Rev. Earth Planet. Sci. 26, 23–51.
Nimmo, F. et al., 2008. Implications of an impact origin for the martian hemispheric dichotomy. Nature 453, 1220–1223.
O'Keefe, J.D., Ahrens, T.J., 1977. Impact-induced energy partitioning, melting, and vaporization on terrestrial planets. Lunar Planet. Sci. Conf. VIII, vol. 10, pp. 3357–3374.
O'Neill, H.S.C., Palme, H., 2008. Collisional erosion and the non-chondritic composition of the terrestrial planets. Philos. Trans. R. Soc. A 366, 4205–4238.
Pham, L.B.S., 2012. Habitability of Mars, Effects of Asteroidal and Cometary Impacts on the Atmospheric Mass Evolution and Implications on Climate During the Late Noachian Period. Ph.D. thesis. Royal Observatory of Belgium.
Pham, L.B.S., Karatekin, O., Dehant, V., 2009. Effects of meteorite impacts on the atmospheric evolution of Mars. Astrobiology 9 (1), 45–54.
Pham, L.B.S., Karatekin, O., Dehant, V., 2011. Effects of impacts on the atmospheric evolution: Comparison between Mars, Earth and Venus. Planet. Space Sci. 59, 1087–1092.
Phillips, R.J., Bullock, M.A., Hauck II, S.A., 2001. Climate and interior coupled evolution on Venus. Geophys. Res. Lett. 28, 1779–1782.
Pierazzo, E., Vickery, A.M., Melosh, H.J., 1997. A reevaluation of impact melt production. Icarus 127, 408–423.
Rampino, M.R., 1987. Impact cratering and flood basalt volcanism. Nature 327, 468.
Raymond, S.N. et al., 2013. Dynamical and collisional constraints on a stochastic late veneer on the terrestrial planets. Icarus 226, 671–681.
Reese, C.C., Orth, C.P., Solomatov, V.S., 2010. Impact origin for the martian crustal dichotomy: Half-emptied or half-filled? J. Geophys. Res. 115 E05004.
Reese, C.C., Solomatov, V.S., Orth, C.P., 2007. Mechanisms for cessation of magmatic resurfacing on Venus. J. Geophys. Res. 112. http://dx.doi.org/10.1029/2006JE002782 E04S04.
Reese, C.C. et al., 2004. Magmatic evolution of the impact-induced martian mantle plumes and the origin of Tharsis. J. Geophys. Res. 109 E08009.
Ribas, I. et al., 2005. Evolution of the solar activity over time and effects on planetary atmospheres. I. High-energy irradiances (1–1700 Å). Astrophys. J. 622, 680–694.
Ribas, I. et al., 2010. Evolution of the solar activity over time and effects on planetary atmospheres. II. κ1 Ceti, an analog of the Sun when life arose on Earth. Astrophys. J. 714, 384–395.
Rivera-Valentin, E.G., Barr, A., 2014. Impact-induced compositional variations on Mercury. Earth Planet. Sci. Lett. 391, 234–242.
Roberts, J.H., Barnouin, O.S., 2012. The effect of the Caloris impact on the mantle dynamics and volcanism of Mercury. J. Geophys. Res. 117 E02007.
Ronca, L.B., 1966. Meteoritic impact and volcanism. Icarus 5, 515–520.
Ryder, G., 2002. Mass flux in the ancient Earth–Moon system and benign implications for the origin of life on Earth. J. Geophys. Res. 107, 6-1–6-13.
Schaber, G.G. et al., 1992. Geology and distribution of impact craters on Venus: What are they telling us? J. Geophys. Res. 97, 13257–13301.
Schlichting, H.E., Sari, R., Yalinewich, A., 2015. Atmospheric mass loss during planet formation: the importance of planetesimal impacts. Icarus 247, 81–94.
Segura, T.L. et al., 2013. The effects of impacts on the climate of terrestrial planets. In: Mackwell, S.J. et al. (Eds.), Comparative Climatology of Terrestrial Planets. Univ. of Arizona, Tucson, pp. 417–437.
Senshu, H., Kuramoto, K., Matsui, T., 2002. Thermal evolution of a growing Mars. J. Geophys. Res. 107, 5118. http://dx.doi.org/10.1029/2001JE001819.
Shuvalov, V., 1999. Multi-dimensional hydrodynamic code SOVA for interfacial flows: Application to the thermal layer effect. Shock Waves 9, 381–390.
Shuvalov, V., 2009. Atmospheric erosion induced by oblique impacts. Meteorit. Planet. Sci. 44, 1095–1105.
Shuvalov, V., 2010. Atmospheric erosion induced by oblique impacts. Lunar Planet. Sci. XLI. Extended Abstract #1191.
Shuvalov, V., Trubetskaya, I.A., 2007. Aerial burst in the terrestrial atmosphere. Solar Syst. Res. 41, 220–230.
Shuvalov, V. et al., 2014. Impact induced erosion of hot and dense atmospheres. Planet. Space Sci. 98, 120–127.
Smith, D.S., Scalo, J., Wheeler, J.G., 2004. Transport of ionizing radiation in terrestrial-like exoplanet atmospheres. Icarus 171, 229–253.
Solomon, S.C., Bullock, M.A., Grinspoon, D.H., 1999. Climate change as a regulator of tectonics on Venus. Science 286, 87–90.
Strom, R.G., Schaber, G.G., Dawson, D.D., 1994. The global resurfacing of Venus. J. Geophys. Res. 99, 10899–10926.
Svetsov, V.V., 2000. On the efficiency of the impact mechanism of atmospheric erosion. Solar Syst. Res. 34, 398–410.
Svetsov, V.V., 2007. Atmospheric erosion and replenishment induced by impacts of cosmic bodies upon the Earth and Mars. Solar Syst. Res. 41, 28–41.
Svetsov, V.V., 2011. Simulation of early martian atmosphere controlled by impacts. Planet. Inst. Sci. Conf. Abstracts 1137.
Tackley, P.J., 1996. Effects of strongly variable viscosity on three-dimensional compressible convection in planetary mantles. J. Geophys. Res. 101, 3311–3332.
Tackley, P.J., 1998. Three-dimensional simulations of mantle convection with a thermochemical CMB boundary layer: D? In: Gurnis, M., Wysession, M.E., Knittle, E., Buffett, B.A. (Eds.), The Core–Mantle Boundary Region. American Geophysical Union, pp. 231–253.
Tackley, P.J., 2008. Modelling compressible mantle convection with large viscosity contrasts in a three-dimensional spherical shell using the yin-yang grid. Phys. Earth Planet. Int. 171, 7–18.
Tackley, P.J., 2015. Intrusive magmatism on Venus can lead to a weak crust and episodic overturn events: Spherical 2D and 3D simulations. Geophys. Res. Abs. 17, EGU2015-13804.
van Thienen, P., Vlaar, N.J., van den Berg, A.P., 2004. Plate tectonics on the terrestrial planets. Phys. Earth Planet. Int. 142, 61–74.
Tsiganis, K. et al., 2005. Origin of the orbital architecture of the giant planets of the Solar System. Nature 435, 459–461.
Turcotte, D.L., 1995. How does Venus lose heat? J. Geophys. Res. 100, 16931–16940.
Turtle, E.P., Pierazzo, E., O'Brien, D.P., 2003. Numerical modeling of impact heating and cooling of the Vredefort impact structure. Meteorit. Planet. Sci. 38, 293–303.
Vickery, A.M., 1990. Impacts and atmospheric erosion on the early Earth. LPI Contrib. 746, 51–52.
Walker, J.C.G., 1986. Impact erosion of planetary atmospheres. Icarus 68, 87–98.
Xie, S., Tackley, P.J., 2004. Evolution of helium and argon isotopes in a convecting mantle. Phys. Earth Planet. Int. 146, 417–439.
Yamazaki, D., Karato, S., 2001. Some mineral physics constraints on the rheology and geothermal structure of Earth's lower mantle. Am. Mineral. 86, 385–391.
Zahnle, K.J., Kasting, J.F., 1986. Mass fractionation during transonic escape and implications for loss of water from Mars and Venus. Icarus 68, 462–480.
Zahnle, K.J., Kasting, J.F., Pollack, J.B., 1988. Evolution of a steam atmosphere during Earth's Accretion. Icarus 74, 62–97.
Zahnle, K.J., Pollack, J.B., Grinspoon, D., 1992. Impact generated atmospheres over Titan, Ganymede, and Callisto. Icarus 95, 1–23.
Zahnle, K. et al., 2007. Emergence of a habitable planet. Space Sci. Rev. 129, 35–78.
Zhang, M.H.G. et al., 1993. The ancient oxygen atmosphere of Mars: Implications for atmosphere evolution. J. Geophys. Res. 98, 10915–10923.